Crop Protection 155 (2022) 105921

Contents lists available at ScienceDirect

Crop Protection

journal homepage: www.elsevier.com/locate/cropro

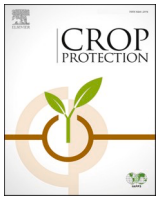

The effect of fan setting, air-conveyor orientation and nozzle configuration on airblast sprayer efficiency: Insights relevant to trellised vineyards

Marco Grella [a,*], Paolo Marucco [a], Ingrid Zwertvaegher [b], Fabrizio Gioelli [a], Claudio Bozzer [a], Alessandro Biglia [a], Marco Manzone [a], Amedeo Caffini [c], Spyros Fountas [d], David Nuyttens [b], Paolo Balsari [a]

[a] Department of Agricultural, Forest and Food Sciences (DiSAFA), University of Turin (UNITO), Largo Paolo Braccini, 2, 10095, Grugliasco, (TO), Italy
[b] Flanders Research Institute for Agriculture, Fisheries and Food (ILVO), Burgemeester Van Gansberghelaan 115, Bus 1, 9820, Merelbeke, Belgium
[c] Caffini S.p.a., Via Guglielmo Marconi, 2, 37050, Palù, (VR), Italy
[d] Agricultural University of Athens (AUA), Iera Odos 75, 11845, Athens, Greece

ARTICLE INFO

Keywords:
Pesticide application
Airflow characterization
Air deflectors
Nozzles
Vertical spray profile
Vertical patternator
Spray technology
3D crop

ABSTRACT

A step-by-step laboratory procedure was used to identify the optimal configuration of a tower-shaped trailed sprayer intended for application in vertical shoot trellised vineyards. Different fan settings, air-conveyor orientation, and nozzle configuration were tested for their effect on both airflow pattern and vertical spray distribution. The optimal airflow rate at the fan outlet and the airflow velocity pattern at crop target distance were identified for different fan settings obtained by the combination of two fan gear speeds and three Power Take Off speeds (450, 500 and 540 rev min^{-1}). The difference in the airflow pattern between factory air deflector settings and the adjusted ones was tested. Once the optimal fan setting was selected, the use of 12 or 16 active nozzles and 4 nozzle types was also tested. The optimal vertical spray profiles were determined based on defined thresholds of i) coefficient of variation, ii) amount of spray liquid lost above the target height and iii) two symmetry indices. The low fan gear speed combined with PTO set at 450 rev min^{-1} result in the best option to reduce and obtain adequate air velocities. The adjustment of deflectors allowed to exactly match the spray to the canopy target height. Concurrently, the use of 12 nozzles drastically reduced the spray losses above the target height. Finally, 4 configurations out of 18, featured by the combination of a different nozzle type and number of active nozzles, met all the criteria set for optimal vertical spray profile.

1. Introduction

The objective of pesticide applications is to deliver the minimum amount of active ingredient to achieve the desired biological effect, precisely, uniformly and exclusively to the target (Giles and Comino, 1989). Although challenging, pesticide losses, under- and over-application, as well as inadequate coverage and deposition, should be avoided as much as possible to safeguard the environment, food safety and human health.

Among the negative side effects of plant protection products (PPP) use, agrochemical spray drift continues to be a major challenge because pesticides can be deposited in undesirable areas and pose risks to both the environment and bystanders (Butler Ellis et al., 2010; Felsot et al., 2011; Grella et al., 2017; Kasner et al., 2020). Spray drift is a larger risk in bush/tree crops than in arable field crops (Rautmann et al., 2001). In orchards, spray is directed sideways and upward into the canopy by means of air-assistance. Therefore, drift not only includes droplets that move horizontally through the canopy and beyond, but also droplets that move vertically above the canopy (via direct spraying into the air or via upward diffusion from the sprayed canopy) and into the atmosphere. Most spray drift thus involves droplets that move above the canopy for part or all of their pathway (Miller et al., 2003). Any improvement to spray application efficiency can potentially contribute to agricultural sustainability in three ways: (i) reduce environmental and human contamination risk, (ii) improve PPP benefit, and (iii) raise food quality and safety standards.

In recent years, efforts have focused on improving the design of pesticide application equipment. Nevertheless, although many developments have focused on sensor-based precision spraying to maximize treatment efficacy and minimize the risks of pesticide off-target

* Corresponding author.
E-mail address: marco.grella@unito.it (M. Grella).

https://doi.org/10.1016/j.cropro.2022.105921
Received 11 August 2021; Received in revised form 18 January 2022; Accepted 19 January 2022
Available online 31 January 2022
0261-2194/© 2022 The Authors. Published by Elsevier Ltd. This is an open access article under the CC BY-NC-ND license (http://creativecommons.org/licenses/by-nc-nd/4.0/).

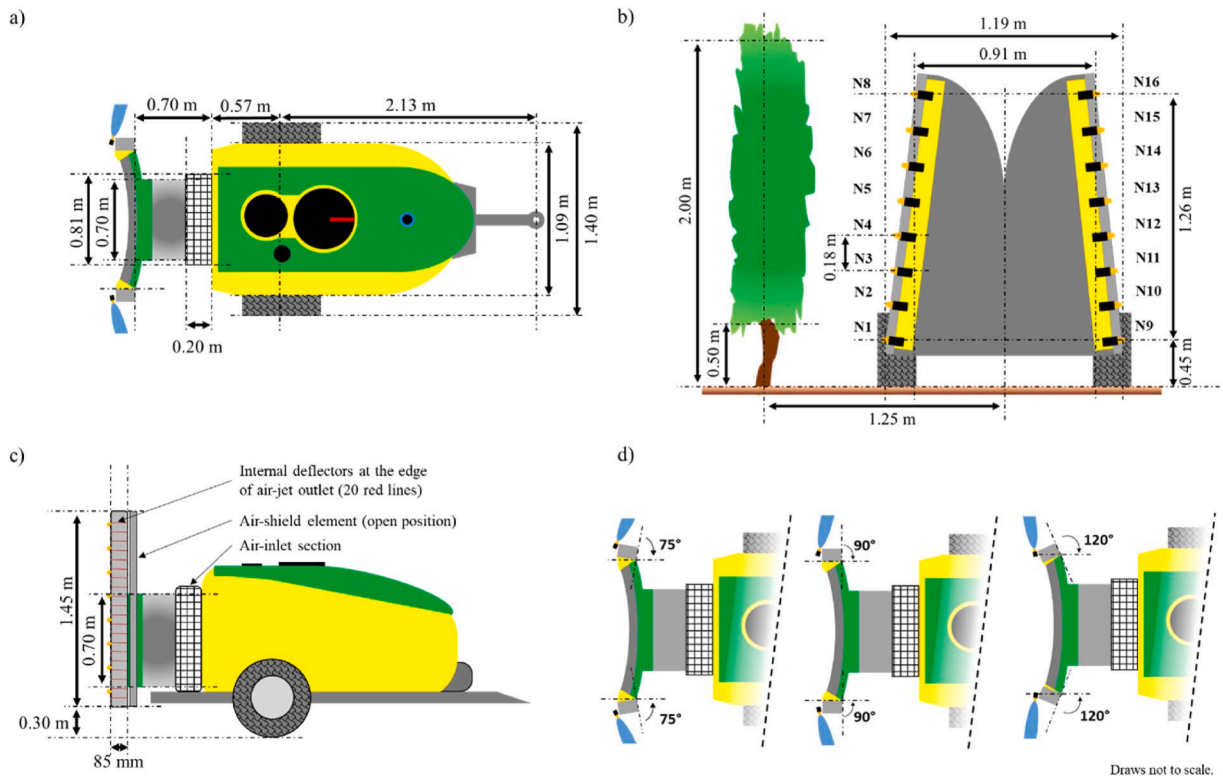

Fig. 1. Caffini Synthesis vineyard sprayer featured by a tower shaped air-jet discharge system with multiple manually adjustable deflectors placed internally at the edge of the air-jet outlet, and electrically-swivelling air-conveyor, (a) aerial view, (b) rear view, (c) side view, and (d) different air-conveyor orientations (forward, orthogonal, and backward, at 75°, 120° and 90° with respect to the central axis of the air-jet discharge system, respectively).

losses (Gil et al., 2007; Doruchowski et al., 2009; Llorens et al., 2010; Berk et al., 2016; Hołownicki et al., 2017; Li et al., 2018; Campos et al., 2019; Comba et al., 2020; Deng et al., 2020; Mammarella et al., 2020; Salcedo et al., 2020b), the gap between these novel high-end crop protection solutions and everyday European agricultural practices remains significant (Gil et al., 2020). Indeed, a recent inventory conducted among vine growers in Italy underlines that the sprayers used by farmers are characterized by a low-technology level (Marucco et al., 2019). Therefore, the correct sprayer setting, and thus the right sprayer adjustment according to the treatment specification, is still key in all PPP treatments to optimise efficacy and reduce environmental impact (Grella et al., 2021; Pascuzzi et al., 2018) and consequently to reach a more sustainable agriculture that pays attention to the environment, bystanders and consumers by reducing chemical inputs according to the European Green Deal, Farm to Fork Strategy (EC,2020). Operator training and improving the farmer's skills and experience about sprayer optimization remain the most effective way for an efficient spray application. Sprayer optimization includes an array of adjustments made to the sprayer to maximize the spray deposition on the intended target (e.g., canopy or fruit) and to minimize spray losses due to drift and to the ground (Hoheisel et al., 2020).

In vineyards, a wide range of sprayer equipment is used for applying PPP, such as manually operated sprayers (Sánchez-Hermosilla et al., 2012), knapsack mist blowers, directed nozzle hydraulic and pneumatic sprayers (Cerruto, 2007; Grella et al., 2020), electrostatic spray technologies (Salcedo et al., 2020a), airblast sprayers, over-row sprayers (Pergher et al., 2013; Balsari et al., 2018), tunnel sprayers with or without air assistance, as well as aerial applications (Panneton et al., 2005). However, most vineyard sprayers are equipped with axial fans producing an outgoing radial current, although in some regions pneumatic sprayers featuring a centrifugal fan are frequently used (Codis et al., 2015; Marucco et al., 2019). Axial fans are preferred for their airflows of great volume and low velocity that penetrate the canopies more effectively than those of lower volume and higher velocity (Randall, 1971; Triloff, 2015). Using conventional airblast sprayers, spray drift and losses to the soil can be as high as 85% (Viret et al., 2003). One of the main aspects reducing spray losses in vineyard and orchard applications is matching spray and air–assistance patterns from the sprayer to the existing canopy (Bahlol et al., 2019) as the sprayed liquid follows the direction of the airflow (Dekeyser et al., 2013; van de Zande et al., 2017). According to Gil et al. (2013), an adequate adjustment of spray liquid distribution to the canopy structure can reduce spray drift up to 90% and reduce pesticide use up to 20%.

The vertical spray distribution pattern depends among other factors on spray pressure, air support, and fan rotational speed, but especially on nozzle configuration, including nozzle type, nozzle orientation, nozzle-to-nozzle distance and distance from the target surface (Farooq and Landers, 2004; Godyn et al., 2014; Wegener et al., 2016). Vertical patternators, which intercept the spray jet while allowing the airflow to pass, are generally used to assess the spray distribution profile, and to adjust the sprayer settings to the canopy (Biocca and Gallo, 2014; Gil et al., 2013; Pergher, 2004). The spray liquid distribution is directly linked to the generated airflow pattern and the airflow characteristics (Dekeyser et al., 2013; Vereecke et al., 2000). Proper adjustment of airflow thus plays a key role in the efficiency of spray application (Vereecke et al., 2000). In recent years, various studies have focused on the strong effect of airflow characteristics on canopy deposition and off-target losses (Lander, 2010; Salcedo et al., 2019; Grella et al., 2020).

Air assistance is used to enhance transport of droplets in the canopy by moving and lifting the foliage and thus to improve spray penetration, deposition and coverage, including on the underside of leaves (Farooq and Salyani, 2002; Cross et al., 2003; Viret et al., 2003; Salcedo et al., 2015a). However, inappropriate design and fan settings can have a negative effect on spray distribution, spray losses and deposition (Świechowski et al., 2004; Dekeyser et al., 2014; Triloff, 2015). For example, excessive air velocities may blow the droplets through the

Table 1
Main characteristics tested for the fan airflow pattern measurements.

ID unique[a]	Fan gear speed	Power Take Off (rev min^{-1})	Deflectors adjusted	Air-conveyor orientation[b]
SP_L450_orth	Low	450	No	Orthogonal
SP_L500_orth	Low	500	No	Orthogonal
SP_L540_orth	Low	540	No	Orthogonal
SP_H450_orth	High	450	No	Orthogonal
SP_H500_orth	High	500	No	Orthogonal
SP_H540_orth	High	540	No	Orthogonal
Adj_L450_forw	Low	450	Yes	Forward
Adj_L450_orth	Low	450	Yes	Orthogonal
Adj_L450_back	Low	450	Yes	Backward

[a] ID unique is composed of deflectors adjustment (SP = "Starting Point" not adjusted; Adj = Adjusted to match the canopy target), fan settings namely fan gear speed (L = Low; H = High) together with PTO (450, 500 or 540 rev min^{-1}) and air-conveyor orientation (forw = forward; orth = orthogonal; back = backward).

[b] Forward, orthogonal and backward orientation corresponding to 75°, 90° and 120° relative to the central axis of the air-conveyor.

trees owing to canopy compression, thus increasing spray losses (Vereecke et al., 2000; Friso et al., 2015) and reducing canopy deposition (Pergher, 2006; Li et al., 2021). Furthermore, the canopy characteristics and geometry (tree size, shape, density, growth stage, distance between trees and rows, training system) also impact the spray coverage (Vereecke et al., 2000) and the incidence of spray drift (Balsari and Marucco, 2004). Sprayer optimization adjustments should therefore be based on knowledge of the crop characteristics and the air-assisted spray pattern.

Conventional axial fan sprayers generally only have a few options for adjusting the airflow pattern and vertical spray distribution. Typically, the air adjustment is based on the rotational speed of the fan and on the position of air deflectors which impact air velocity and air direction, respectively (Marucco et al., 2008). For spray distribution, the number of nozzles and the nozzle type may vary, while the position of the nozzles relative to the fan outlet is usually fixed.

Usually, researchers focus their investigation on the spray equipment calibration and adjustment on either i) the liquid spray pattern (Gil et al., 2013; Pascuzzi, 2016) or ii) the fan airflow pattern through dedicated measurements and complex CFD models (Badules, et al, 2018; Delele et al., 2007; Salcedo et al., 2021). As mentioned before, the spray liquid distribution is directly linked to the generated airflow pattern and the airflow characteristics, so an overall optimization of spray and airflow patterns generated by the airblast sprayers must be considered concurrently. In this respect, Bahlol et al. (2019, 2020) recently developed a patternator able to simultaneously perform liquid and fan airflow measurements. The device was compared with a conventional vertical patternator by Rathnayake et al. (2021).

The objective of this study was to determine under controlled laboratory conditions the fan settings, air-conveyor-orientation and nozzles configuration to obtain the optimal fan airflow pattern and vertical spray profile relevant to spray application in mechanized commercial vertical shoot trellised vineyard (Intrieri and Poni, 1995; Grella et al., 2019, 2021; Pergher and Petris, 2008; Vitali et al., 2013).

2. Materials and methods

A series of laboratory trials were performed at the Crop Protection Technology laboratory (DiSAFA, UNITO) to measure the i) fan airflow and ii) vertical spray profile to determine the optimal sprayer settings relevant to spray application in vertical shoot trellised vineyard, hypothetically featured by 2.5 m inter-row distance and vines characterized by a continuous vegetative strip between 0.5 m and 2.0 m height above the ground at full growth stage. Full growth stage is generally from BBCH 71 to 89, accounting for the growth season period where the vegetative strip is fully developed and shaped through canopy management techniques such as shoot trimming, positioning and tying (Intrieri and Poni, 1995; Lorenz et al., 1995). The fan airflow rate, the fan airflow pattern and the vertical spray profile were evaluated using a step-by-step procedure.

2.1. Sprayer characteristics

A trailed airblast vineyard sprayer, Caffini Synthesis (Caffini S.p.a., Palù, Verona, IT), featured by an 800 L polyethylene tank, was used (Fig. 1a). The sprayer was equipped with a 700 mm diameter fan, consisting of nine blades rotating anticlockwise, and a two-speed gearbox, enabling variable airflow rate according to the speed gearbox selected. The air was sucked in from the front of the tower-shaped air-conveyor. Per sprayer side, the air-conveyor was equipped with 20 manually adjustable deflectors placed internally at the edge of the air-jet outlet, thus allowing to direct the airflow to match the canopy height (Fig. 1c). An electric-control allowed variation of the orientation of the air-conveyor in a range of 15° forward up to 30° backward with respect to the central axis of the air-jet discharge system, thus determining the incidence angle of both airflow and spray jets on the canopy (Fig. 1d). Per sprayer side, eight double nozzle holders, at a fixed position relative to the air-conveyor, were placed at 180 mm spacing (Fig. 1b).

2.2. Fan airflow rate

2.2.1. Fan settings and experimental set-up

The airflow rate (m^3 h^{-1}) generated by the sprayer was determined at two fan gear-box speeds (high vs. low) and three tractor Power Take Off (PTO) settings (450, 500 and 540 rev min^{-1}), resulting in six airflow settings. The PTO was set and checked during the trials through the tractor (New Holland T4040V; CNH Industrial, Turin, Italy) digital tachometer (±1 rev min^{-1}). In all cases, the air-conveyor was maintained orthogonal (90° relative to the central axis of the air-jet discharge system, Fig. 1d).

The air velocity was measured at the air-jet outlet in a sampling grid covering the whole outlet section of the tower-shaped air-conveyor, similar to the methodology employed by Garcerá et al. (2017). Per sprayer side, the air-conveyor was divided into 21 equally distributed sections by the deflectors placed inside. Each subsection corresponded to 5865 mm^2 (69 mm height x 85 mm width) and contained three measuring points equally distributed along its diagonal (Figure A1a) to cover possible differences in air velocity, resulting in 63 measuring points per sprayer side.

A stainless-steel Pitot-tube probe, measuring 500 mm length and 7 mm diameter (accuracy 0.09 and 0.27 m s^{-1} at 5 and 15 m s^{-1}, respectively), connected to a Testo 400 device (Testo SE & Co. KGaA, Titisee-Neustadt, DE) was used to measure the air velocity. An ad hoc support was used to maintain the probe perpendicular to the ground in a fixed position throughout the measurements. In each measuring point, the air velocity was recorded at a frequency of 1 Hz for 60 s and averaged over the recording period. Per section, the average of the 3 measuring points was determined.

The rotational speed of the fan (rev min^{-1}) was measured simultaneously using an optical tachometer for contact-free measuring via laser (Jaquet DHO907; Jaquet Technology Group AG, Pratteln, CH). Data were collected during 60 s and then averaged.

2.2.2. Data analysis

The total airflow rate Q_{tot} (m^3 h^{-1}) was calculated according to Eq. (1):

$$Q_{tot} = 3,600 \times \sum_{i=1}^{21} \left[(V_i \times S_i)_r + (V_i \times S_i)_l \right] \quad (1)$$

where Q_{tot} (m^3 h^{-1}) is the total airflow generated by the sprayer; i is the corresponding section at the air-conveyor outlet (1–21 from bottom to

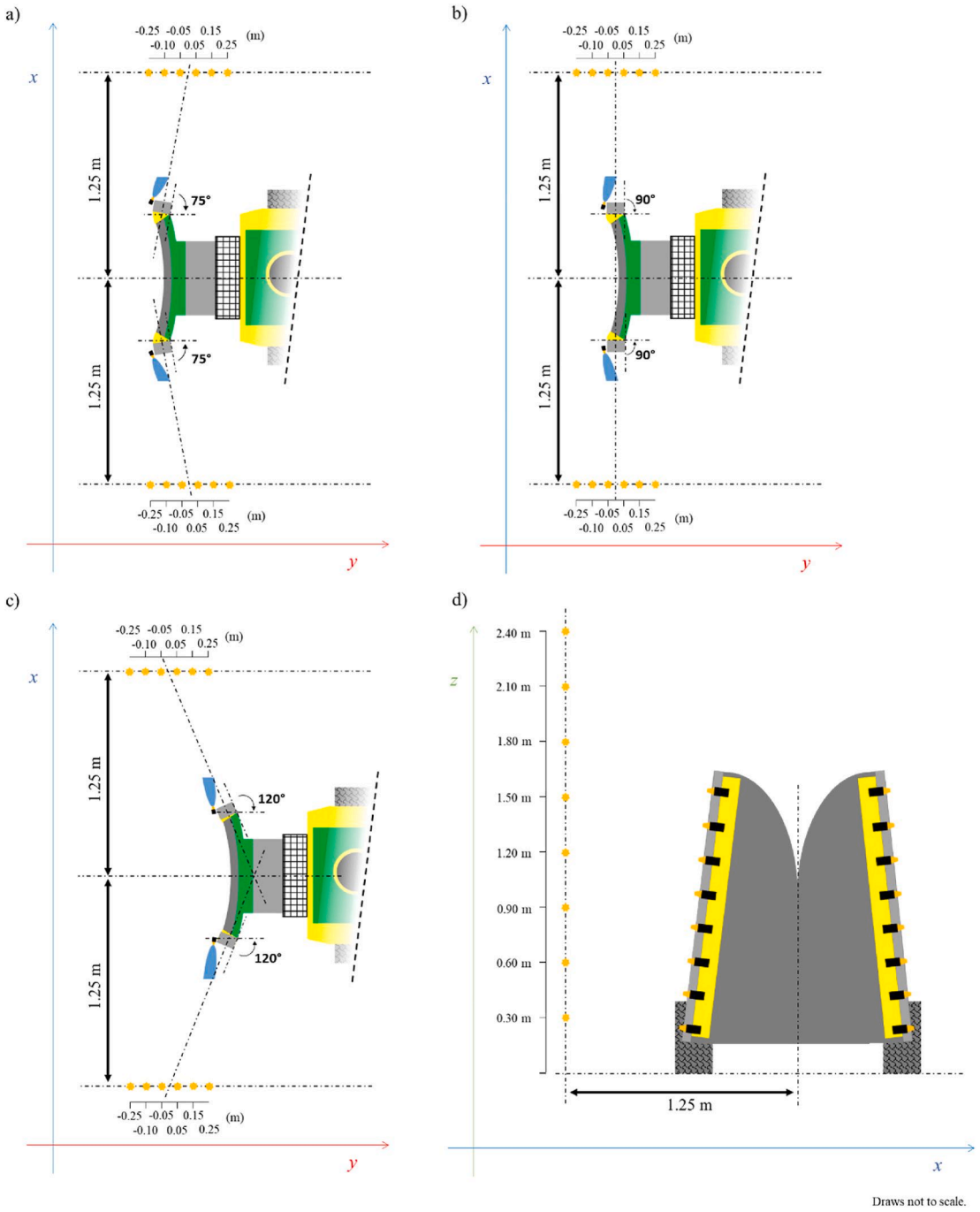

Fig. 2. Layout of the airflow pattern measuring points relative to the (a) forward, (b) orthogonal and (c) backward air-conveyor orientation, and (d) to the height above the ground and distance to the central axis of the sprayer (2.5 m inter-row distance was considered).

top); V_i (m s^{-1}) is the average air velocity of section i; S_i (m^2) is the surface of section i; r and l are the right and left side of the sprayer, respectively.

The airflow rate was characterized for each air conveyor section, from the bottom to the top (Figure A1a), and the symmetry between sprayer sides (i.e. % of airflow rate per side) was evaluated per each configuration. In addition, linear regression was used to determine the relationship between the fan rotational speed (rev min^{-1}) and total airflow rate (m^3 h^{-1}).

2.3. Fan airflow pattern

2.3.1. Fan settings, air-conveyor orientation and experimental set-up

First, the airflow pattern generated by the sprayer with the deflectors at standard factory or starting point settings was evaluated (Table A1). The same six airflow settings as for the airflow rate measurements, i.e. a combination of high or low fan gear-box speed with a PTO of 450, 500, or 540 rev min^{-1}, were tested, while keeping the air-conveyor in an orthogonal position (Fig. 1d).

Based on these first results, the setting with low fan gear speed at 450 rev min^{-1} PTO was selected for a second round of trials in which the internal air deflectors were adequately adjusted to match the target. The adjustment of air deflectors consisted of varying the angle of each

Table 2
Main characteristics tested for the vertical spray profile measurements. All configurations were tested using the Power Take Off set at 450 rev min^{-1} with low fan gear speed. In all cases, the air deflectors were adjusted to match the canopy target.

ID unique[a]	Nozzles type(s)	Number of active nozzles[b]	Total flow rate (l min^{-1})[c]	Air-conveyor orientation[d]
HC_16_orth	TXB8002	8 + 8	14.56	Orthogonal
FF_16_orth	XR8002	8 + 8	14.56	Orthogonal
AI_16_orth	AI8002	8 + 8	14.56	Orthogonal
HC_12_orth	TXB8002	6 + 6	10.92	Orthogonal
HC_12_forw	TXB8002	6 + 6	10.92	Forward
HC_12_back	TXB8002	6 + 6	10.92	Backward
FF_12_orth	XR8002	6 + 6	10.92	Orthogonal
FF_12_forw	XR8002	6 + 6	10.92	Forward
FF_12_back	XR8002	6 + 6	10.92	Backward
AI_12_orth	AI8002	6 + 6	10.92	Orthogonal
AI_12_forw	AI8002	6 + 6	10.92	Forward
AI_12_back	AI8002	6 + 6	10.92	Backward
FF-OC_12_orth	(XR8002 + UB8502)	(4 + 2)+(4 + 2)	10.92	Orthogonal
FF-OC_12_forw	(XR8002 + UB8502)	(4 + 2)+(4 + 2)	10.92	Forward
FF-OC_12_back	(XR8002 + UB8502)	(4 + 2)+(4 + 2)	10.92	Backward
AI-OC_12_orth	(AI8002 + AIUB8502)	(4 + 2)+(4 + 2)	10.92	Orthogonal
AI-OC_12_forw	(AI8002 + AIUB8502)	(4 + 2)+(4 + 2)	10.92	Forward
AI-OC_12_back	(AI8002 + AIUB8502)	(4 + 2)+(4 + 2)	10.92	Backward

[a] ID unique configuration is composed of nozzle type (HC = hollow cone; FF = flat fan; AI = Air Inclusion flat fan; OC = off-center), number of activated nozzles (12 or 16) and air-conveyor orientation (forw = forward; orth = orthogonal; back = backward).
[b] Left + right sprayer side.
[c] Total nominal flow rate at a constant liquid pressure of 0.4 MPa.
[d] Forward, orthogonal and backward orientation corresponding to 75°, 90° and 120° relative to the central axis of the air-conveyor.

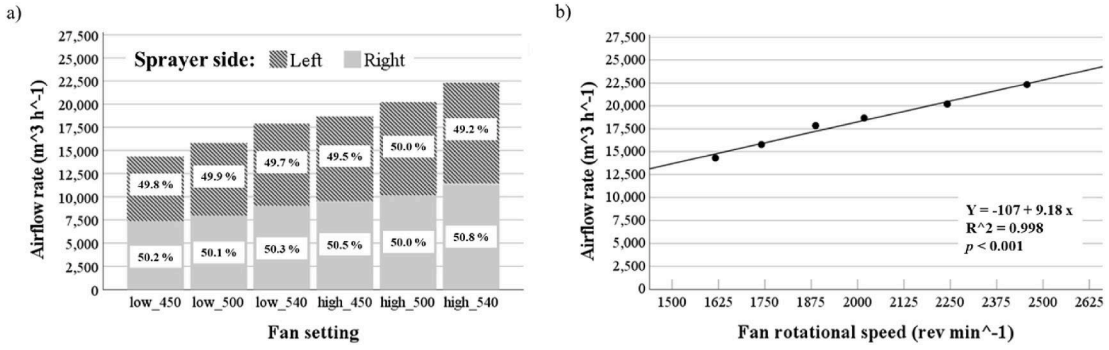

Fig. 3. (a) Airflow rate (m^3 h^{-1}) generated by the axial fan on the right (light grey) and left (dark grey) sprayer side for the different combinations of fan gear speed (low and high) and Power Take Off setting (450, 500 and 540 rev min^{-1}). (b) Linear regression of fan rotational speed (rev min^{-1}) and average airflow rate (m^3 h^{-1}).

deflector from its original starting point position, in order to match the direction of the fan air-jet to the canopy target height and to avoid airflow exceeding the canopy height (Table A1). To adjust the deflectors, a goniometer was used to set the right-angle position of each one, which were then attached to the main air-conveyor frame using screws (Figure A1b). In these trials, three air-conveyor orientations (Fig. 1d, max forward, orthogonal and max backward, i.e. respectively 75°, 90°, and 120° relative to the central axis of the air-jet discharge system) were tested. An overview of the tested configurations is given in Table 1.

The airflow pattern measurements were conducted in the middle of a warehouse at least 8 m distance from its walls, ensuring that neither the walls nor the tractor affected the air currents behaviour in the sampling area. Outdoor windows and doors were kept open to minimize air overpressure from the walls or other undesirable inner turbulences. To characterize the main current coming from the fan, the airflow velocities and directions were measured statically on both sprayer sides, following a 2D sampling grid scheme (Fig. 2). Preliminary trials were conducted to evaluate the main direction of the generated air stream, considering that in most cases it cannot be perpendicular to the fan outlet orientation (Salcedo et al., 2015a, 2019; Triloff, 2016; van de Zande et al., 2017). The measurements were performed using a sonic anemometer Gill 2D1 (Gill instruments LTD., Lymington, UK) mounted on a support at a distance of 1.25 m from the centre of the sprayer, thus simulating an inter-row distance of 2.5 m. Due to the short distance between the fan outlet and the sampling grid position on the X axis (range of 0.66 and 0.80 m due to the air-conveyor tower shape), the airflow deviation from the perpendicular was considered negligible. Therefore, the sampling grid was always centred and aligned with the central axis of the air-conveyor, irrespective of its orientation, namely forward, orthogonal or backward (Fig. 2a, b and 2c). On the Z axis, measurements were taken at 8 positions (300 mm steps) from 0.30 m to 2.40 m above the ground (Fig. 2d). On the Y axis, measurements were taken at 6 positions (100 mm steps) from −0.25 m to 0.25 m from the centre of the air-conveyor (Fig. 2a, b, and 2c). Measurements were thus conducted in 48 positions along a grid of 2.10 m high and 0.50 m long. The probe was automatically shifted from one measuring point to another on the Y and Z axes (accuracy of positioning system ± 2 mm) through a hydraulically driven movable support. The airflow velocities and directions on the Y and Z

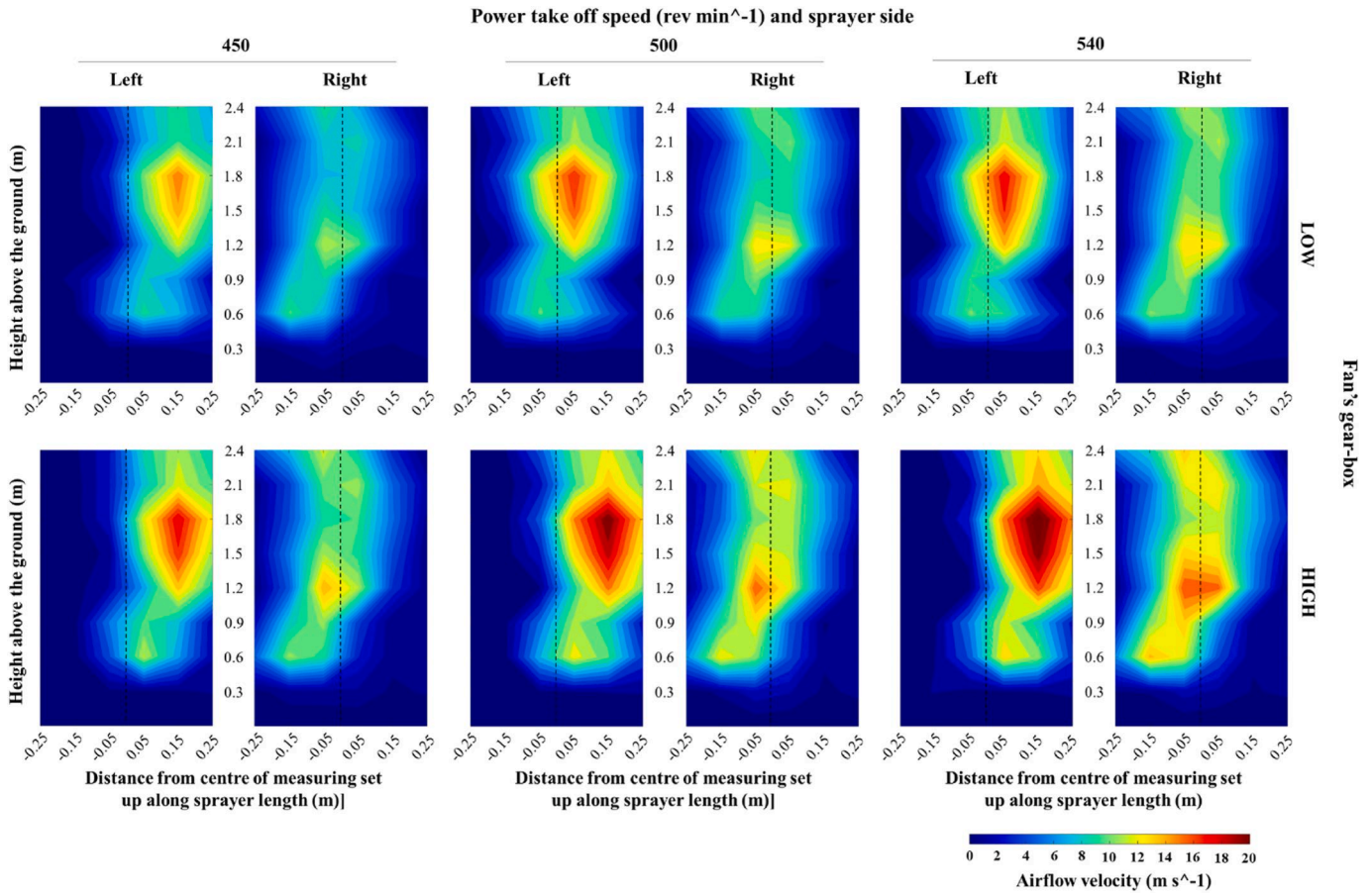

Fig. 4. Colours maps of airflow velocity (m s^{-1}) at the target (1.25 m from the central axis of the sprayer) for the right and left sprayer sides and for each combination of fan gear speed (low and high) and Power Take Off settings (450, 500 and 540 rev min^{-1}). In all cases, the air-conveyor was oriented orthogonal and the air deflectors were not adjusted to match the canopy target (starting point). The black dashed line represents the central axis of the air-conveyor. (For interpretation of the references to colour in this figure legend, the reader is referred to the Web version of this article.)

Table 3
Results of the four-way ANOVA ($p < 0.05$) for the airflow velocity (m s^{-1}) measured at the target (1.25 m from the central axis of the sprayer) including configurations featured by orthogonal air-conveyor orientation and air deflectors not adjusted to match the canopy target.

Sources	DF[a]	$p>(F)$	Significance[b]
Main effects			
Power Take Off (PTO)	2	0.072	NS
Fan gear speed (FGS)	1	0.030	*
Sprayer side (SS)	1	0.394	NS
Height above the ground (H)	7	1.61E-13	***
Interactions			
PTO x FGS	2	0.958	NS
PTO x SS	2	0.947	NS
PTO x H	14	1.000	NS
FGS x SS	1	0.656	NS
FGS x H	7	0.999	NS
SS x H	7	0.317	NS
PTO x FGS x SS	2	0.968	NS
PTO x FGS x H	14	1.000	NS
PTO x SS x H	14	1.000	NS
FGS x SS x H	7	1.000	NS
PTO x FGS x SS x H	14	1.000	NS

[a] DF error = 480.
[b] Statistical significance level: NS p > 0.05; * p < 0.05; ** p < 0.01; *** p < 0.001.

axes were recorded for 60 s at a frequency of 1 Hz and then averaged.

2.3.2. Data analysis

All statistical analyses were performed using IBM SPSS Statistics (Version 27) predictive analytics software for Windows. The data were tested for normality using the Shapiro-Wilk test and by visual assessment of the Q-Q plots of Z-scores; residuals analyses were also performed.

To test the effect of the fan settings on the airflow velocity, a four-way ANOVA was performed with PTO (450, 500 and 540 rev min^{-1}), fan gear speed (high and low), sprayer side (left and right) and height above the ground as independent variables. In addition, to test the effect of air deflectors adjustment on the airflow velocity, a three-way ANOVA was used with deflector adjustment ("staring point" and adjusted), sprayer side (left and right) and height above the ground. Finally, the effect of air-conveyor orientation on the airflow velocity was tested using a three-way ANOVA including air-conveyor orientation (backward, orthogonal and forward), sprayer side (left and right) and height above the ground. In all cases, the interactions among factors were investigated and the means were compared using a Duncan post-hoc test for multiple comparison ($p < 0.05$). To investigate the airflow patterns obtained with the different sprayer configurations at the target distance, 2D air velocity colour-maps and 2D quiver plots displaying the air direction vectors (U) and air velocity vectors (V), were generated using Matlab® R2020a.

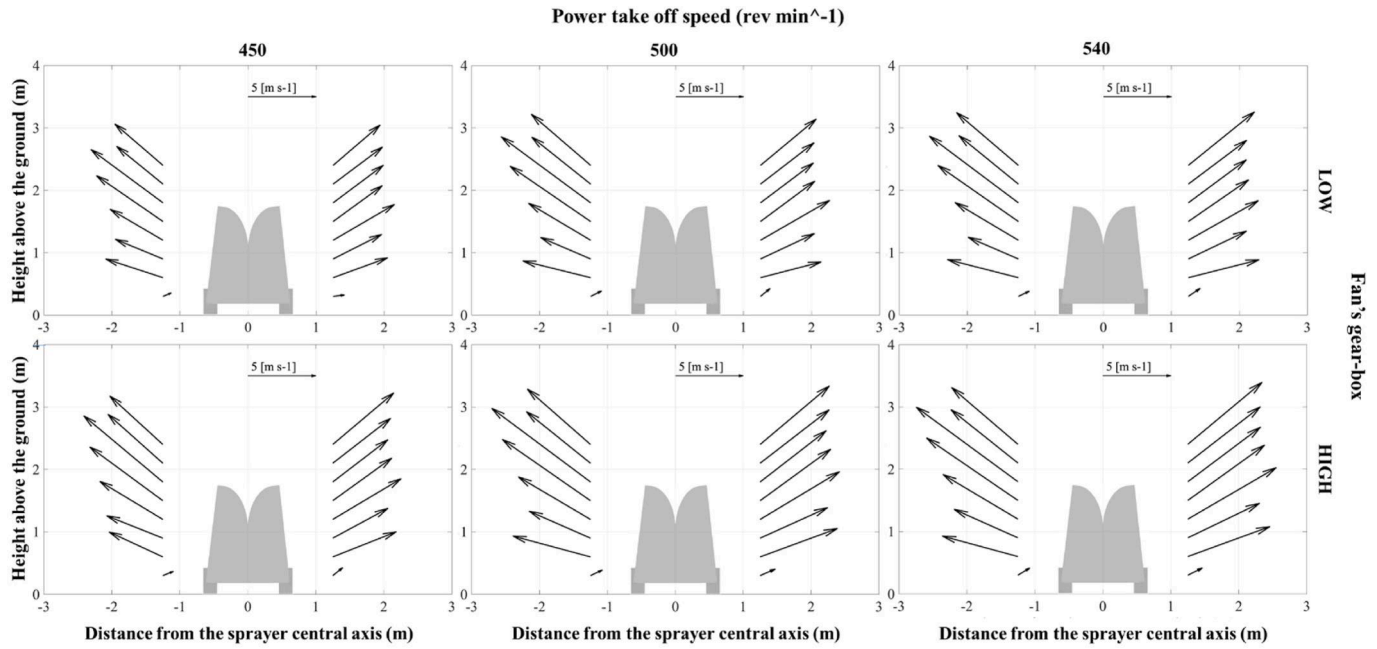

Fig. 5. Air velocity vectors on ZX planes for both sprayer sides at the target (1.25 m from the central axis of the sprayer) and for each combination of fan gear speed (low and high) and Power Take Off settings (450, 500 and 540 rev min^{-1}). In all cases, the air-conveyor was oriented orthogonal and the air deflectors were not adjusted to match the canopy target (starting point).

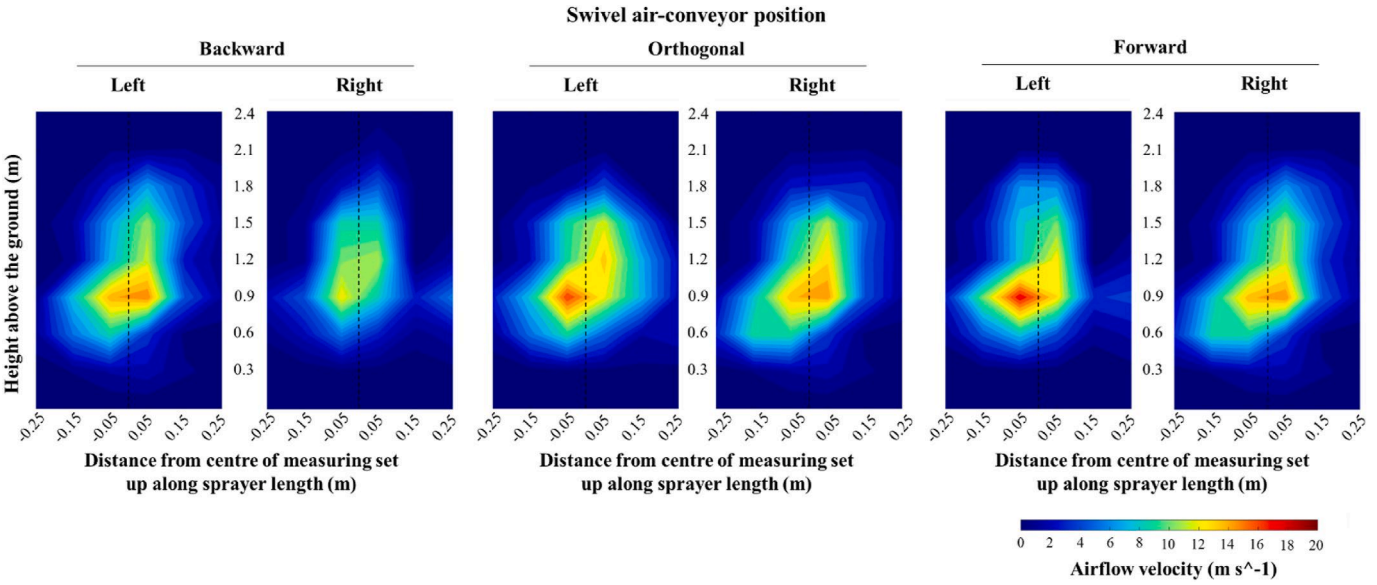

Fig. 6. Colours maps of airflow velocity (m s^{-1}) at the target (1.25 m from the central axis of the sprayer) for different air-conveyor orientations (backward, orthogonal and forward). In all cases, the low fan gear speed, 450 rev min^{-1} Power Take Off, and the air deflectors properly adjusted to match the canopy target, were used. The black dashed line represents the central axis of the air-conveyor. (For interpretation of the references to colour in this figure legend, the reader is referred to the Web version of this article.)

2.4. Vertical spray profile

2.4.1. Sprayer configurations and experimental set-up

To determine the optimal sprayer configurations for the specified trellised vineyard, the vertical spray distribution of 18 configurations, consisting of a combination of nozzle type (hollow cone TXB 80 02, flat fan XR 80 02, air inclusion flat fan AI 80 02, off-centre flat fan UB-85 02, off-centre air-inclusion flat fan AIUB 85 02; TeeJet, Spraying Systems Co., Wheaton, Illinois USA), number of active nozzles (12, 16), and air-conveyor orientation (forward, backward, orthogonal) were tested. An overview of the tested configurations is given in Table 2.

All configurations were tested at 450 rev min^{-1} PTO, low fan gear speed, and with air deflectors adjusted to the canopy (as described above). In the configurations consisting of a combination of standard and off-centre nozzles, the off-centre nozzles were mounted in the positions N1, N6, N9 and N14 (Fig. 1d). To achieve an applied volume rate in the range of 400–600 l ha^{-1}, in accordance to farmers' practices (Marucco et al., 2019), ISO 02 nozzles at 0.4 MPa pressure, corresponding to a nominal nozzle flow rate of 0.91 l min^{-1}, and a sprayer forward speed of 5.5 km h^{-1} (1.53 m s^{-1}) were used. With a total number of active nozzles of 12 and 16, volume rates of 477 and 635 l ha^{-1} were achieved, respectively.

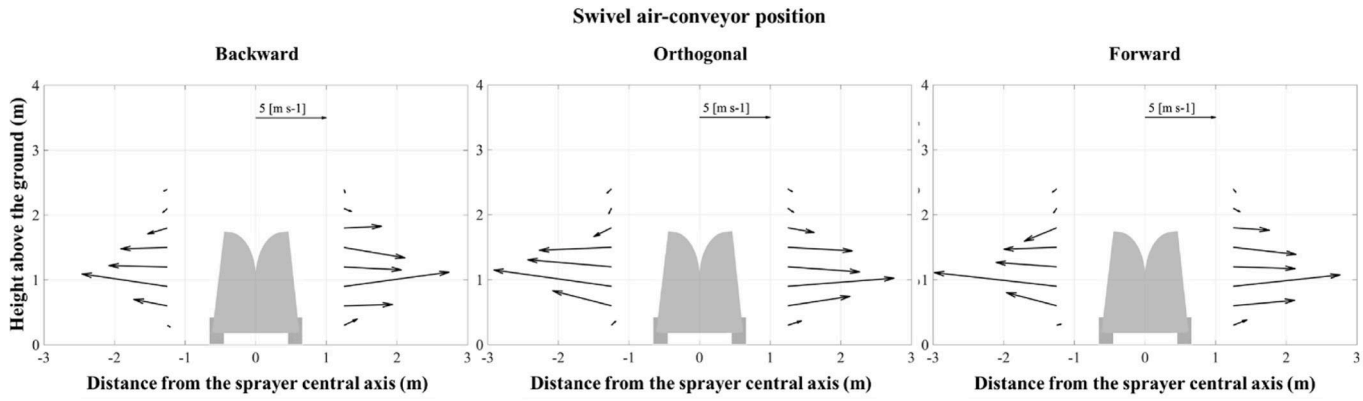

Fig. 7. Air velocity vectors on ZX planes for both sprayer sides at the target (1.25 m from the central axis of the sprayer) and for different air-conveyor orientations (backward, orthogonal and forward). In all cases, the low fan gear speed, 450 rev min^{-1} Power Take Off, and the air deflectors properly adjusted to match the canopy target, were used.

Table 4
Results of the three-way ANOVA ($p < 0.05$) for the airflow velocity (m s^{-1}) measured at the target (1.25 m from the central axis of the sprayer) including configurations featured by low fan gear speed and 450 rev min^{-1} Power Take Off.

Sources	DF[a]	p>(F)	Significance[b]
Main effects			
Air deflectors position (AD)	1	0.048	*
Sprayer side (SS)	1	0.675	NS
Height above the ground (H)	7	1.55E-05	***
Interactions			
AD x SS	1	0.860	NS
AD x H	7	6.82E-04	***
SS x H	7	0.999	NS
AD x SS x H	7	0.990	NS

[a] DF error = 160.
[b] Statistical significance level: NS p > 0.05; * p < 0.05; ** p < 0.01; *** p < 0.001.

Table 5
Results of the three-way ANOVA ($p < 0.05$) for the airflow velocity (m s^{-1}) measured at the target (1.25 m from the central axis of the sprayer) including configurations featured by low fan gear speed, 450 rev min^{-1} Power Take Off and air deflectors adjusted to match the canopy target.

Sources	DF[a]	p>(F)	Significance[b]
Main effects			
Air-conveyor orientation (AC)	2	0.445	NS
Sprayer side (SS)	1	0.553	NS
Height above the ground (H)	7	6.91E-22	***
Interactions			
AC x SS	2	0.692	NS
AC x H	14	0.999	NS
SS x H	7	0.997	NS
AC x SS x H	14	1.000	NS

[a] DF error = 240.
[b] Statistical significance level: NS p > 0.05; * p < 0.05; ** p < 0.01; *** p < 0.001.

The trials were performed using a vertical patternator with discs (AAMS-Salvarani BVBA, Maldegem, BE). The patternator consisted of an aluminium frame on which water collecting trays with ridges were mounted. The trays were characterized by an exposed surface of 0.20 m × 0.20 m and were positioned every 0.20 m along the vertical axis in two staggered arrays. The middle of the bottom tray was located at 0.50 m above the ground (liquid collection from 0.40 to 0.60 m), while the top tray was located at 3.10 m height (liquid collection from 3.00 to 3.20 m). Thus, the patternator collected the spray liquid from 0.40 m up to 3.20 m in 14 discrete measuring points within the vertical spray profile. Once collected, the trays led the spray liquid through hoses to a 100 ml graduated cylinder where the volume was automatically measured and recorded through an integrated ultrasonic system. Similar as for the airflow measurements, the patternator was mounted on an electrically driven rail at a distance of 1.25 m from the central axis of the sprayer to simulate an inter-row distance of 2.5 m. Measurements consisted of passing four times in front of the static sprayer at a forward speed of 0.4 km h^{-1} (0.11 m s^{-1}). Per pass, the patternator went completely out of the spray cloud in order to properly collect the liquid over the entire spray length. For each tested configuration (Table 2), three repetitions were performed per sprayer side.

2.4.2. Data analysis

The vertical spray profiles of the tested configurations, representing the percentage of liquid collected (%) at different heights above the ground (m) relative to the total volume collected by the patternator, were evaluated based on the assumption that the optimal spray distribution consists of a uniform deposition over the entire target zone (from 0.5 m to 2.0 m height), with a good symmetry between sprayer sides, with a minimum spray deposition or spray loss below and above the target zone. Different assessment parameters were used:

i) The amount of spray liquid collected above the target height SL_{out} (ml) was calculated using Eq. (2). The lower this amount, the lower the potential environmental impact of the tested spray configuration. Although the spray losses below the target are also interesting for their direct impact on the ground losses, it was not possible to measure the liquid below 0.5 m due to the technical characteristics of the patternator.

$$SL_{out} = 0.5 \times \sum_{i=9}^{14} \left[(SL_i)_r + (SL_i)_l \right] \quad (2)$$

where SL_{out} (ml) is the amount of liquid collected above the target height averaged over both sprayer sides; i is the corresponding patternator tray (trays 9 to 14 are located out of the target height); SL_i is the amount of liquid (ml) recovered by tray i; r and l are the right and left side of the sprayer, respectively.

ii) The average coefficient of variation CV_{avg} (%) was calculated according to Eq. (3). The lower the CV_{avg}, the more uniform the spray liquid collected by the patternator at different heights in the range of the target height.

$$CV_{avg} = 0.5 \times \left[\left(\frac{\sigma}{\mu} \right)_r + \left(\frac{\sigma}{\mu} \right)_l \right] \times 100 \quad (3)$$

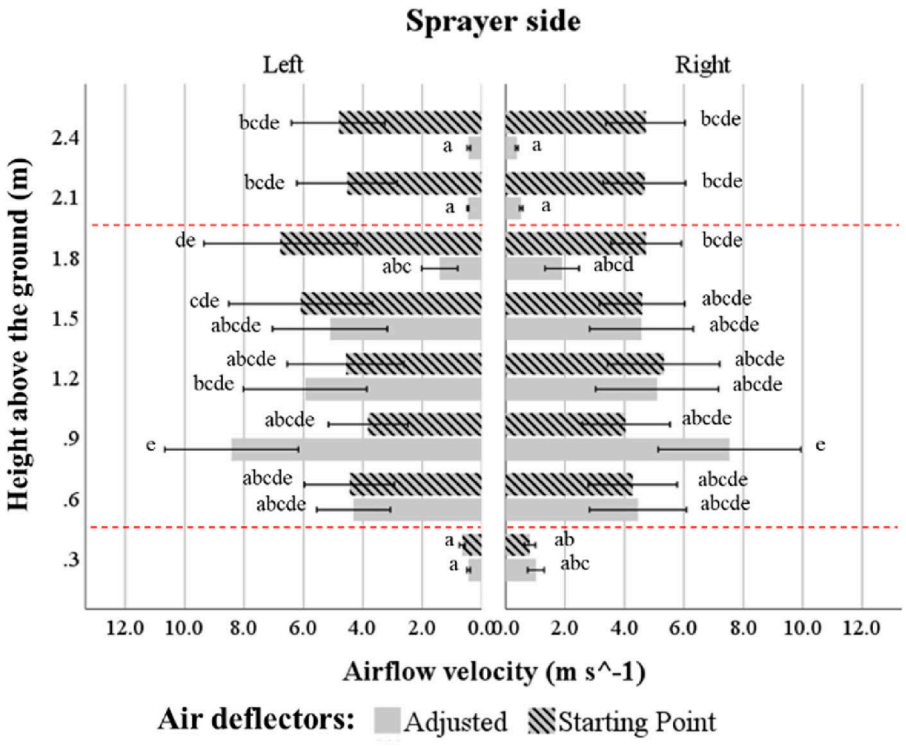

Fig. 8. Air velocity (m s^{-1}) at the target (1.25 m from the central axis of the sprayer) and at different heights above the ground for the right and left sprayer side, using the air deflectors not adjusted (starting point) and adjusted to match the canopy target. In all cases, the low fan gear speed, 450 rev min^{-1} Power Take Off, and the orthogonal air-conveyor orientation, were used. The red dashed lines represent the lower (0.5 m) and upper border (2.0 m) of the canopy target. The bars show the mean ± standard error of the mean. Different letters denote significant differences between average airflow velocities measured at different heights, all against all where letters are common across both sides (Duncan post hoc test, $p < 0.05$). (For interpretation of the references to colour in this figure legend, the reader is referred to the Web version of this article.)

where CV_{avg} (%) is the coefficient of variation averaged over both sprayer sides; μ is the mean liquid (ml) collected by the patternator trays located in the range of the target height (trays 1 to 8); σ is the standard deviation of the mean; *r* and *l* are the right and left side of the sprayer, respectively.

iii) Symmetry index *SA* (%), which is similar to the index used by Gil et al. (2013), was calculated using Eq. (4). The higher *SA*, the better the symmetry. In addition, a second symmetry index *SB* (adim.) was calculated following Eq. (5). The lower *SB*, the better the symmetry. Two symmetry indexes were used as they have different sensitivity in detect symmetry between sprayer sides.

$$SA = \left(1 - \sum_{i=1}^{8} \left| - \left(\frac{SL_i}{\sum_{i=1}^{8} SL_i}\right)_r + \left(\frac{SL_i}{\sum_{i=1}^{8} SL_i}\right)_l \right| \right) * 100 \quad (4)$$

$$SB = \sum_{i=1}^{8} \left| 0.5 \times \frac{-(SL_i)_r + (SL_i)_l}{(SL_i)_r + (SL_i)_l} \right| \quad (5)$$

where *SA* (%) is symmetry index A; *SB* (adim.) is symmetry index B; *i* is the corresponding patternator tray (trays 1 to 8 are located in the range of the target height); SL_i is the amount of liquid (ml) recovered by tray *i*; *r* and *l* are the right and left side of the sprayer, respectively.

Per tested configuration, the four parameters (SL_{out}, CV_{avg}, *SA* and *SB*) were calculated. Per parameter, the median value of the tested configurations was determined and considered as criteria threshold for optimal vertical spray distribution. Then, all configurations were ranked according to how many criteria they met, from four (optimal) to zero (worst).

3. Results and discussion

3.1. Fan airflow rate

The increase in PTO rotational speed from 450 to 540 rev min^{-1} showed a linear increase in total airflow rate (Fig. 3a) for both high and low fan gear speed. The high fan gear speed always generated the highest total airflow rate, irrespective of PTO rotation (Fig. 3a). The average airflow rate generated using the low fan gear speed was 14,315, 15,783, and 17,851 $m^3 h^{-1}$, whereas with the high fan gear speed it was 18,705, 20,204, and 22,332 $m^3 h^{-1}$ with PTOs set at 450, 500 and 540 rev min^{-1}, respectively. In general, incremental steps in airflow rate were thus observed from lowest values at 450 rev min^{-1} PTO with low fan gear speed to highest at 540 rev min^{-1} PTO with high fan gear speed. The incremental behaviour can be explained by the linear relationship between the generated airflow rate and the fan rotational speed ($R^2 = 0.998$; Fig. 3b).

Interestingly, a very high symmetry in airflow rate among both sprayer sides was observed. Indeed, the largest deviation from the perfect symmetry (50% of airflow rate at each side) was merely 0.8% (high_540; Fig. 3a). A slightly higher airflow rate was generally found on the right sprayer side. These findings confirm the benefits of tower-shaped air-conveyors in smoothing the asymmetric character of axial fans (Salcedo et al., 2019) by distributing homogenous airflow rates at both sprayer sides and at different heights (Triloff, 2015). However, the vertical airflow rate profile (Figure A2) showed a tendency of higher values in the top-half of the left side of the air-conveyor, resulting in airflow rate differences along the canopy height mainly on the left side. These differences were most extensive at the high fan gear speed, while they were slight at the low speed. The airflow rates measured on the right sprayer side were uniform over the air-conveyor height (Figure A2). According to Salcedo et al. (2019), the velocities were higher on the left sprayer side owing to the anticlockwise rotation of the fan which provided more energy to this side.

3.2. Fan airflow pattern

Fig. 4 illustrates the airflow velocities (m s^{-1}) measured at the target distance for the different fan settings at the starting point deflector settings (Table A1). In general, the airflow velocities were not distributed equally along the canopy target height. This is confirmed by the significant effect of height above the ground (Table 3). The average airflow velocities do not differ significantly according to the sprayer side

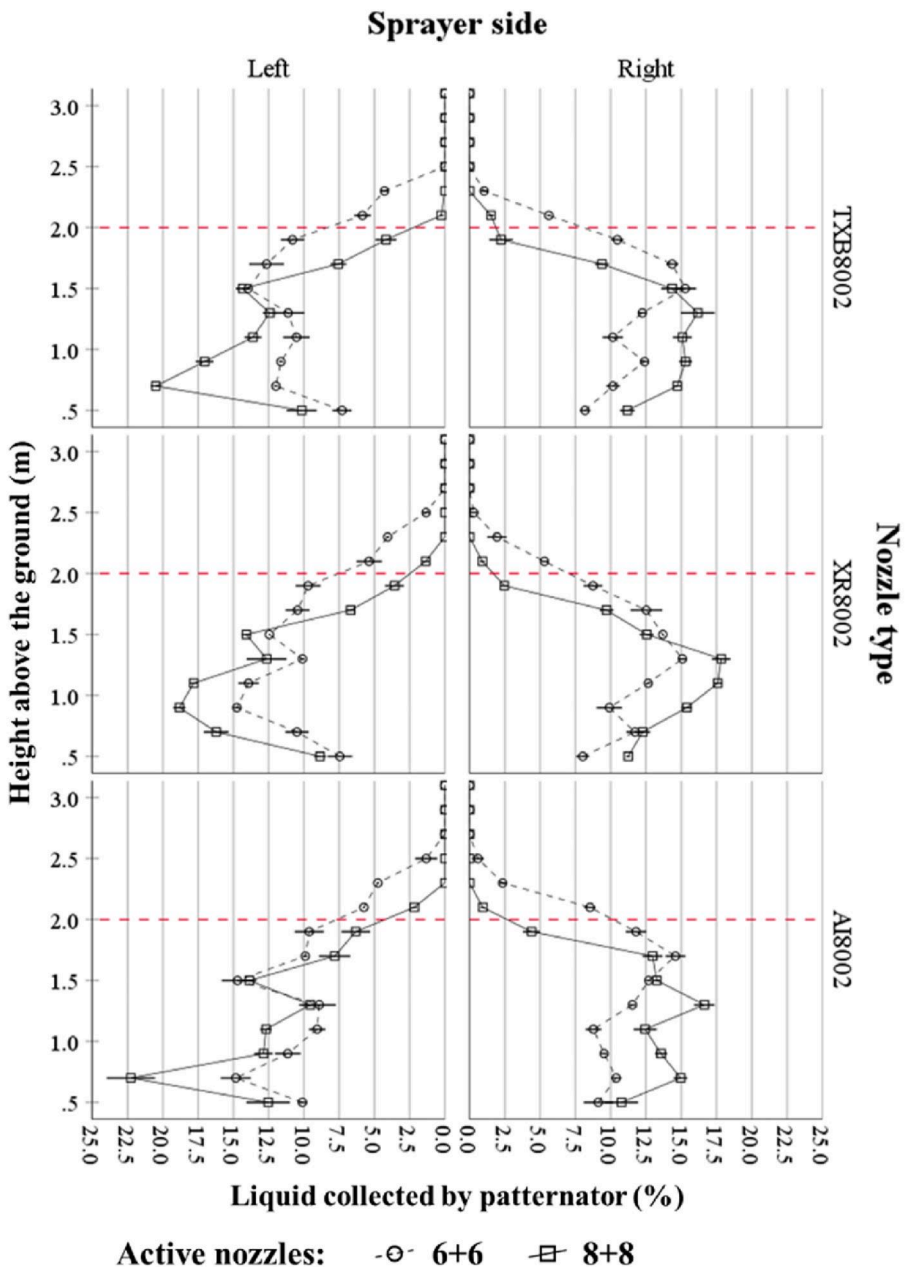

Fig. 9. Vertical spray profiles showing the percentage of liquid collected by the patternator (%) at different heights above the ground (m), relative to the total volume collected. Profiles were obtained at the target (1.25 m from the central axis of the sprayer) for the right and left sprayer side, using 6 or 8 activated nozzles per sprayer side, for different nozzle types. In all cases, the low fan gear speed, 450 rev min^{-1} Power Take Off, the orthogonal air-conveyor orientation, and the air deflectors properly adjusted to match the canopy target, were used. The red dashed lines represent the upper border of the canopy target (2.0 m). The symbols show the mean ± standard error of the mean. (For interpretation of the references to colour in this figure legend, the reader is referred to the Web version of this article.)

(Table 3), probably due to the large variations in airflow velocity along the sprayer length (y axis, Fig. 2). However, on the left sprayer side the maximum air velocity values were always higher than those measured on the right side (Fig. 4). This behaviour can be attributable to the fan rotation direction, as also found by Salcedo et al. (2015b). A trend for increasing airflow velocity with PTO was observed (Fig. 4), even if no significant effect of PTO was detected, while gear speed did have a significant effect (Table 3).

Based on the interpretation of results obtained by Balsari et al. (2008) using an individual spouts airblast sprayer, airflow velocities at the target between 6 and 8 m s^{-1} can be considered as the most suitable to maximize spray deposition and concurrently obtain homogeneous deposits at all canopy parts of a trellised vineyard at middle (BBCH 69) and full (BBCH 77) growth stages (Lorenz et al., 1995). In detail, through field trials, Balsari et al. (2008) found higher canopy depositions at 4 km h^{-1} rather than at 6 and 8 km h^{-1}, but in all cases irrespective of forward speed, higher deposition was achieved using the lower fan settings resulting in airflow velocities at the canopy between 6 and 8 m s^{-1} (statically measured in the laboratory). Excessive air volumes may reduce deposition owing to canopy compression (Hislop, 1991; Pergher, 2006). Based on this threshold, excessive velocities were found for the high fan gear speed configurations with peak values of 18.30, 20.71 and 21.93 m s^{-1} using PTO at 450, 500 and 540 rev min^{-1}, respectively (Fig. 4). At the low fan gear speed, the average airflow velocities measured at the different heights above the ground were not substantially lower than those obtained using the high fan gear speed (Figure A3), but the peak values were reduced to 15.58, 17.11 and 17.83 m s^{-1} at 450, 500 and 540 rev min^{-1}, respectively (Fig. 4). Airflow velocity peaks play an important role because at each height above the ground the airflow exerts its effect with the maximum velocity of that height during the sprayer advancement (Figure A3). In this respect, Svensson (2001) used the maximum air velocity as an expression for how well the air jet was able to penetrate the canopy, namely penetration effectiveness. However, the instantaneous maximum velocity often exhibits great variation and is sensitive to random effects. It should therefore be used with care (Świechowski et al., 2004).

Table 6
Vertical spray profile parameters (mean ± standard deviation), i.e. the coefficient of variation (CV_{avg}, %), amount of liquid above the target height (SL_{out}, ml), symmetry index A (SA, %) and symmetry index B (SB, adim.) for the different sprayer configurations tested. Coloured cells indicate that the threshold for the correspondent parameter is met by the configuration.

ID unique[a]	Parameters used for the evaluation of vertical spray profile				N° of criteria met[b]
	CV_{avg} [%]	SL_{out} [ml]	SA [%]	SB [adim.]	
HC_16_orth	36.02 ± 2.95	24.25 ± 2.7	83.85 ± 1.26	2.59 ± 0.35	3
FF_16_orth	48.11 ± 1.87	19.61 ± 1.84	73.90 ± 1.95	4.51 ± 1.09	1
AI_16_orth	32.44 ± 4.05	19.44 ± 1.77	72.96 ± 4.65	3.50 ± 0.09	1
HC_12_orth	51.50 ± 2.04	4.00 ± 1.00	79.53 ± 0.72	3.84 ± 0.43	1
HC_12_forw	31.15 ± 5.14	0.00 ± 0.00	87.81 ± 2.28	2.28 ± 0.31	4
HC_12_back	43.19 ± 2.47	5.83 ± 1.04	72.38 ± 8.53	2.32 ± 0.55	2
FF_12_orth	52.74 ± 1.36	5.33 ± 0.29	78.18 ± 5.98	2.47 ± 0.95	2
FF_12_forw	43.36 ± 5.43	6.67 ± 2.57	85.43 ± 4.75	2.29 ± 1.06	3
FF_12_back	56.44 ± 3.90	5.92 ± 2.88	83.90 ± 3.69	3.81 ± 0.50	1
AI_12_orth	46.73 ± 3.22	6.33 ± 0.76	72.18 ± 1.10	2.97 ± 0.18	2
AI_12_forw	52.01 ± 3.18	10.25 ± 3.19	74.81 ± 1.32	4.21 ± 0.28	0
AI_12_back	40.88 ± 2.90	13.33 ± 4.07	76.91 ± 10.57	3.15 ± 0.71	2
FF-OC_12_orth	54.69 ± 5.63	3.50 ± 1.32	79.08 ± 3.73	3.99 ± 0.62	1
FF-OC_12_forw	60.96 ± 1.25	2.50 ± 1.50	88.60 ± 4.10	3.53 ± 0.20	2
FF-OC_12_back	57.40 ± 2.55	3.67 ± 1.61	83.90 ± 4.18	3.90 ± 0.28	2
AI-OC_12_orth	54.66 ± 5.33	2.50 ± 1.00	75.96 ± 2.45	3.90 ± 0.42	1
AI-OC_12_forw	40.67 ± 2.57	0.00 ± 0.00	85.26 ± 3.97	1.81 ± 0.52	4
AI-OC_12_back	52.33 ± 4.04	4.33 ± 1.61	78.47 ± 9.02	4.56 ± 0.19	1
Median value[c]	49.69	5.50	79.70	3.46	

[a] ID unique configuration is composed of nozzle type (HC = hollow cone; FF = flat fan; AI = Air Inclusion flat fan; OC = off-center), number of activated nozzles (12 or 16) and air-conveyor orientation (forw = forward; orth = orthogonal; back = backward).
[b] Used to rank the configurations according to the number of criteria met from four (best vertical spray profile) to zero (worst vertical spray profile).
[c] Thresholds used to evaluate the vertical spray profile (CV_{avg}, SL_{out} and SA: lower values = criteria met, SA: higher = criteria met).

Based on the airflow velocity maps (Fig. 4), showing the average air velocity in each sampling point of a 2D spatial grid, the low fan gear speed combined with PTO at 450 rev min^{-1} (SP_L450_orth) can be considered as the most suitable among the configurations tested. At all heights, this configuration obtained velocities above 6 m s^{-1}, in accordance with the thresholds suggested by Balsari et al. (2008). This configuration also resulted in lowest velocity peaks, not exceeding 10 and 15 m s^{-1} on the right and left sprayer side, respectively. Furthermore, configuration SP_L450_orth provided air flow rates (14,800 m^3 h^{-1}) in line with the optimal values found by Pergher and Petris (2008). Those authors demonstrated that airflow rates between 11,500 and 15,000 m^3 h^{-1} were the most suitable to increase deposition in trellised vineyards, whereas higher airflow rates decreased the deposition at all canopy levels. However, the airflow velocity vectors in Fig. 5 show that the starting point settings of the air deflectors did not properly match the canopy height, largely exceeding 2 m height. Furthermore, based on the airflow direction vectors, it can be roughly estimated that 30% of airflow was not used to convey spray droplets into the canopy but was directed upward into the air, thus potentially enhancing spray drift (Triloff, 2015).

Fig. 6 illustrates the airflow pattern of the tower shaped air-conveyor with air deflectors adjusted to match the canopy height, at low fan gear speed and PTO at 450 rev min^{-1}. Irrespective of air-conveyor orientation, the airflow velocities at the target canopy height, i.e. between 0.5 m and 2.0 m above the ground, were higher than 6 m s^{-1}, whereas above 2 m height they abruptly decreased to below 1 m s^{-1}. This was confirmed by the airflow velocity and direction vectors in Fig. 7. At the top of the air-conveyor, the airflow velocities were very low directed towards the centre of the canopy target. The airflow generated by the middle of the air-conveyor showed the highest velocities and was generally perpendicular to the vertical axis and thus directed to the canopy target. The airflow coming from the bottom of the air-conveyor was directed upward toward the target.

Moreover, the air deflector position (starting point vs. adjusted) had a significant effect on airflow velocity (Table 4), underlining that air deflector adjustment not only modifies airflow distribution but also airflow velocities. Considering the significant interaction between air deflector position and height above the ground (Table 4), the increase in airflow velocity compared to the starting point settings can be attributed to a large portion of the total airflow being concentrated to a small canopy section of 1.5 m (Figure A4). No statistical differences were detected between sprayer sides, while airflow velocity was significantly different at different heights above the ground (Table 4).

The airflow velocity maps (Fig. 6) and airflow vectors (Fig. 7) did not show clear effects of the air-conveyor orientation, which acts on the incidence angle of the airflow to the targets as confirmed by the ANOVA (Table 5). Sprayer side was also found to have no significant effect. Height above the ground, however, did significantly affect airflow velocity, confirming the unevenness along the canopy target height, with highest velocities between 0.8 m and 1.0 m above the ground (Figs. 6 and 7). The average velocities measured above 2.0 m target height were significantly lower with the adjusted deflectors than with the starting point configuration. Using the adjusted configuration, the lowest air velocities were obtained above (>2.0 m) and below the target (<0.5 m) thus effectively minimizing the airflow losses beyond the target and resulting in higher airflow velocities focused on the central part of the target between 0.8 and 1.0 m above the ground, as intended (Fig. 8). Using the Point Quadrat Technique, Grella et al. (2019) found a generally higher canopy density at this canopy height corresponding to the grape band, while lower densities were found at the canopy top. Although a uniform airflow throughout the canopy height is generally recommended in a trellised vineyard (TOPPS-Prowadis Project, 2014; Triloff, 2015), the higher airflow velocities at 0.9 m height and the lower velocities at 1.8 m height can be favourable for the spray penetration in accordance with the canopy density, resulting in possible higher deposit and homogeneity throughout the canopy. Nevertheless, lower airflow losses over the target can result in a higher spray deposition as an indirect effect of reduced spray drift losses.

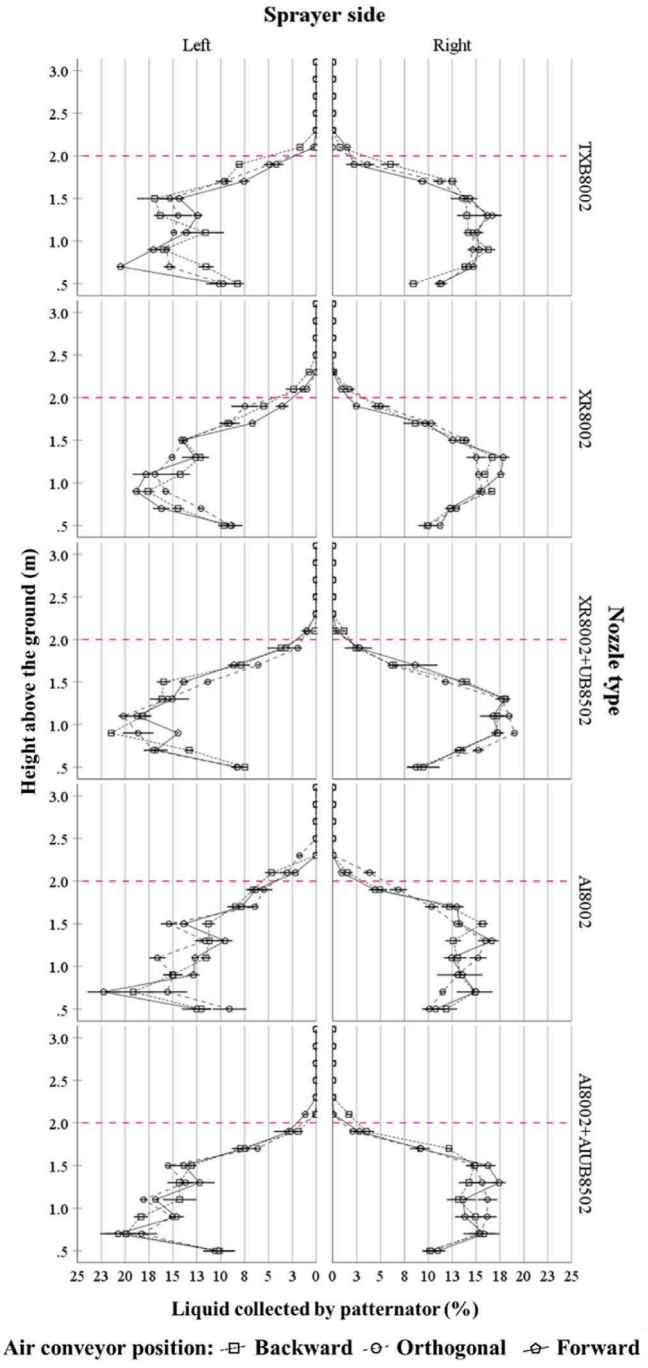

Fig. 10. Vertical spray profiles showing the percentage of liquid collected by the patternator (%) at different heights above the ground (m), relative to the total volume collected. Profiles were obtained at the target (1.25 m from the central axis of the sprayer) for the right and left sprayer side, for different nozzle types and air-conveyor orientations (backward, orthogonal and forward). In all cases, the low fan gear speed, 450 rev min^{-1} Power Take Off, the air deflectors properly adjusted to match the canopy target, and 12 activated nozzles were used. The red dashed lines represent the upper border of the canopy target (2.0 m). The bars show the mean ± standard error of the mean. (For interpretation of the references to colour in this figure legend, the reader is referred to the Web version of this article.)

3.3. Vertical spray profile

Fig. 9 displays the vertical spray profiles obtained by activating six or eight nozzles per sprayer side, using either conventional hollow cone nozzles TXB8002, conventional flat fan nozzles XR8002, or air inclusion nozzles AI8002, with configuration Adj_L450_orth (Table 1). The use of six nozzles per sprayer side reduced the liquid losses above the canopy target and was therefore considered as the best option for further trials. Field trials using an innovative sprayer developed based on the Caffini Synthesis model featured by the same tower shaped air conveyor and pulse width modulation (PWM) spray system with just six nozzles activated, supported the laboratory results of this study (Grella et al., 2021). At 100% PWM duty cycle, corresponding to 0.91 l min^{-1} flow rate per nozzle, the spray coverage measured using water sensitive paper on the top part of the vines, although slightly lower than those measured at the middle and bottom canopy, was adequate to control diseases based on the thresholds provided by Syngenta. However, based on the criteria adopted to select the most optimal configurations, only configurations HC_12_orth and FF_12_orth showed amounts of liquid above the target height which were below the selected threshold (median value SL_{out} = 5.50 ml, Table 6).

Fig. 10 shows the vertical spray profiles of the configurations containing only six active nozzles per sprayer side, including those with off-centre nozzles mounted at the outer positions, at the three different air-conveyor orientations. Within nozzle type, no clear effect of air-conveyor orientation on the percentage of liquid recovered at the different heights from the ground was perceived. Similar, no clear effect of air-conveyor orientation on the spray profile parameters, which allows an objective comparison of the configurations, was observed (Table 6). On the contrary, some differences in vertical spray profiles were detected between the tested sprayer configurations. As expected, the use of off-centre nozzles, both conventional and air inclusion, reduced the spray losses above the target height (SL_{out}) compared to the same configurations without off-centre nozzles. Surprisingly, the coefficients of variation (CV_{avg} %) of the configurations with off-centre nozzles were usually higher than the median (49.69%). Of those configurations, only configuration AI-OC_12_forw met all 4 criteria, with no detectable losses above the target height, low CV_{avg} % and good symmetry of spray liquid between and within sprayer sides, and thus showed the best performance. Configuration HC_12_forw also met all 4 criteria resulting in an optimal spray distribution. In addition, two configurations, i.e. FF_12_forw and HC_16_orth, met all criteria, except the one concerning spray losses outside the target height, making them also good options to obtain optimal vertical spray profiles able to minimize losses and to guarantee good and homogeneous coverage throughout the canopy height.

4. Conclusions

The experimental laboratory trials allowed the identification of the most optimal fan sprayer settings, air-conveyor orientation and nozzle configurations for a spray application in a trellised vineyard using a step-by-step, laboratory-based procedure. From the experimental results it can be concluded that:

i) The airflow generated by the sprayer without air deflector adjustment provided excessive airflow velocities on the target at both high and low fan gear speed. The Power Take Off set to 450 rev min^{-1} allowed to obtain acceptable airflow conditions, namely fan airflow rate below 15,000 m^3 and average air velocities on the target between 6 and 8 m s^{-1}.
ii) The adjustment of multiple air deflectors placed inside the tower shaped air-conveyor plays a key role in properly addressing the fan airflow to match the canopy target height and thus to minimize the spray losses above and beyond the canopy vines with possible positive effects on drift reduction.
iii) The use of six nozzles per sprayer side, instead of eight, reduced the spray losses above the canopy target height, possibly benefiting potential drift reduction.

iv) The definition of four parameters (coefficient of variation, amount of liquid recovered above the target and two symmetry indexes) allowed an objective evaluation of the vertical spray profiles and the identification of the optimal sprayer configurations. These parameters were needed as intuitive selection as a visual assessment of the spray distribution profiles was not straightforward.

v) Based on the vertical spray profiles, four configurations, featured by a combination of nozzle type [conventional hollow cone (HC), conventional flat fan (FF), combination of air inclusion flat fan and off-centre (AI-OC)], number of active nozzles [12 or 16], and air-conveyor orientation [forward (forw) or orthogonal (orth)], were selected as most optimal for spray applications in a trellised vineyard, i.e. HC_12_forw and AI-OC_12_forw meeting 4 criteria, and HC_16_orth and FF_12_forw meeting 3 criteria, respectively.

Field trials in a trellised vineyard at full growth stage are ongoing to validate the selected configurations and settings for their possible effect on spray deposition, coverage, and spray losses (to the air and ground), compared with conventional spray application techniques. Furthermore, ad hoc trials under field conditions are needed to study the effect of air-conveyor orientation on deposition and coverage through its influence of angle incidence on both airflow and spray jet on the canopy target.

Funding

This project has received funding from the European Union's Horizon 2020 research and innovation program under grant agreement No 773718 (OPTIMA-project) http://optima-h2020.eu/.

Declaration of competing interest

The authors declare that they have no known competing financial interests or personal relationships that could have appeared to influence the work reported in this paper.

Acknowledgments

The authors would also like to thank Caffini S.r.l. and TeeJet Technologies for the technical support and materials provided in this research.

Appendix A

Table A1
Angle (°) of the internal deflectors of the air-conveyor at the starting point and the adjusted sprayer setting, for the left and right sprayer side.

Air deflector ID[a]	Deflectors' angle (°)[b]			
	Left	Right	Left	Right
	Starting point[c]		Adjusted[d]	
20	310	50	297	63
19	315	54	298	67
18	309	57	298	64
17	312	56	290	59
16	305	54	290	65
15	311	54	290	64
14	310	60	289	66
13	314	56	289	65
12	312	55	289	65
11	309	59	290	67
10	310	50	292	66
9	312	59	290	66
8	307	59	290	68
7	310	58	290	68
6	300	65	300	65
5	303	72	303	72
4	294	81	294	81
3	290	81	290	81
2	285	80	285	80
1	277	83	277	83

[a] The deflectors are numbered progressively from the bottom to the top of the air-conveyor.
[b] The angle (°) is measured clockwise relative to the vertical Z axis.
[c] Sprayer setting as delivered by the manufacturer without adjustment of air deflectors.
[d] Sprayer setting with air deflectors adjusted to match the canopy target.

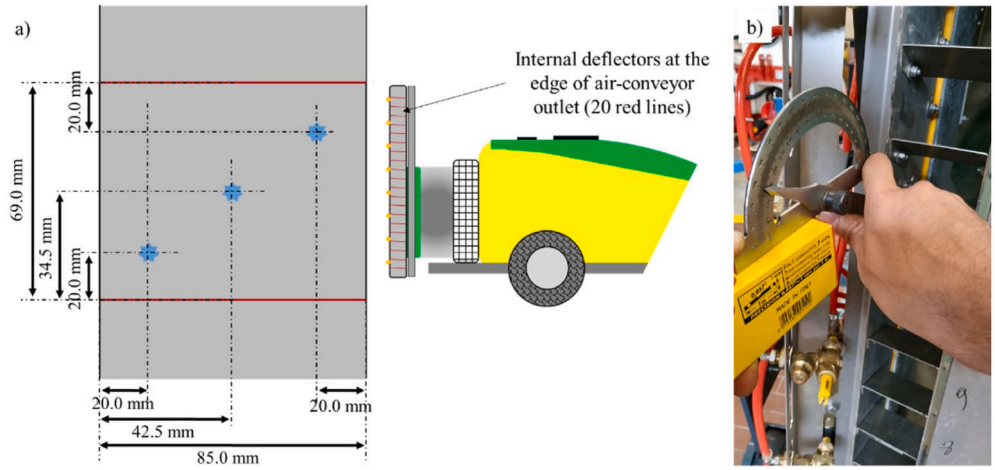

Fig. A1. (a) Detail of air-conveyor section defined by the deflectors (red lines) placed internally at the edge of the air-jet outlet. The light-blue stars indicate the measuring points in each section used for the determination of airflow rate generated by the sprayer. (b) Procedure for the manual adjustment of angle deflectors using a goniometer.

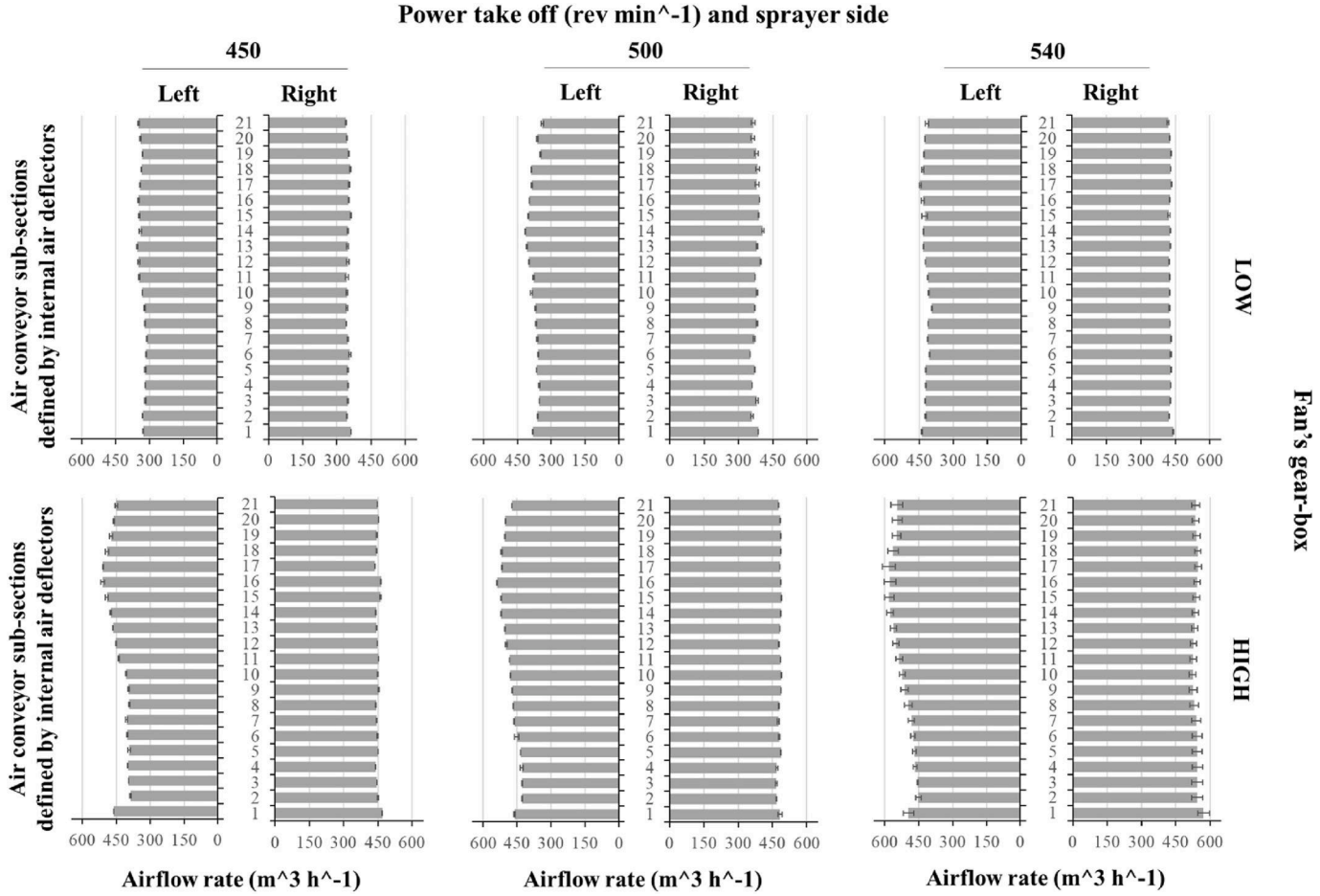

Fig. A2. Airflow rate ($m^3\ h^{-1}$) at the 21 air-conveyor sections, from the bottom (1) to the top (20), for the right and left sprayer side, and for each combination of fan gear speed (low and high) and Power Take Off setting (450, 500 and 540 rev min^{-1}). The bars show the mean ± standard error of the mean.

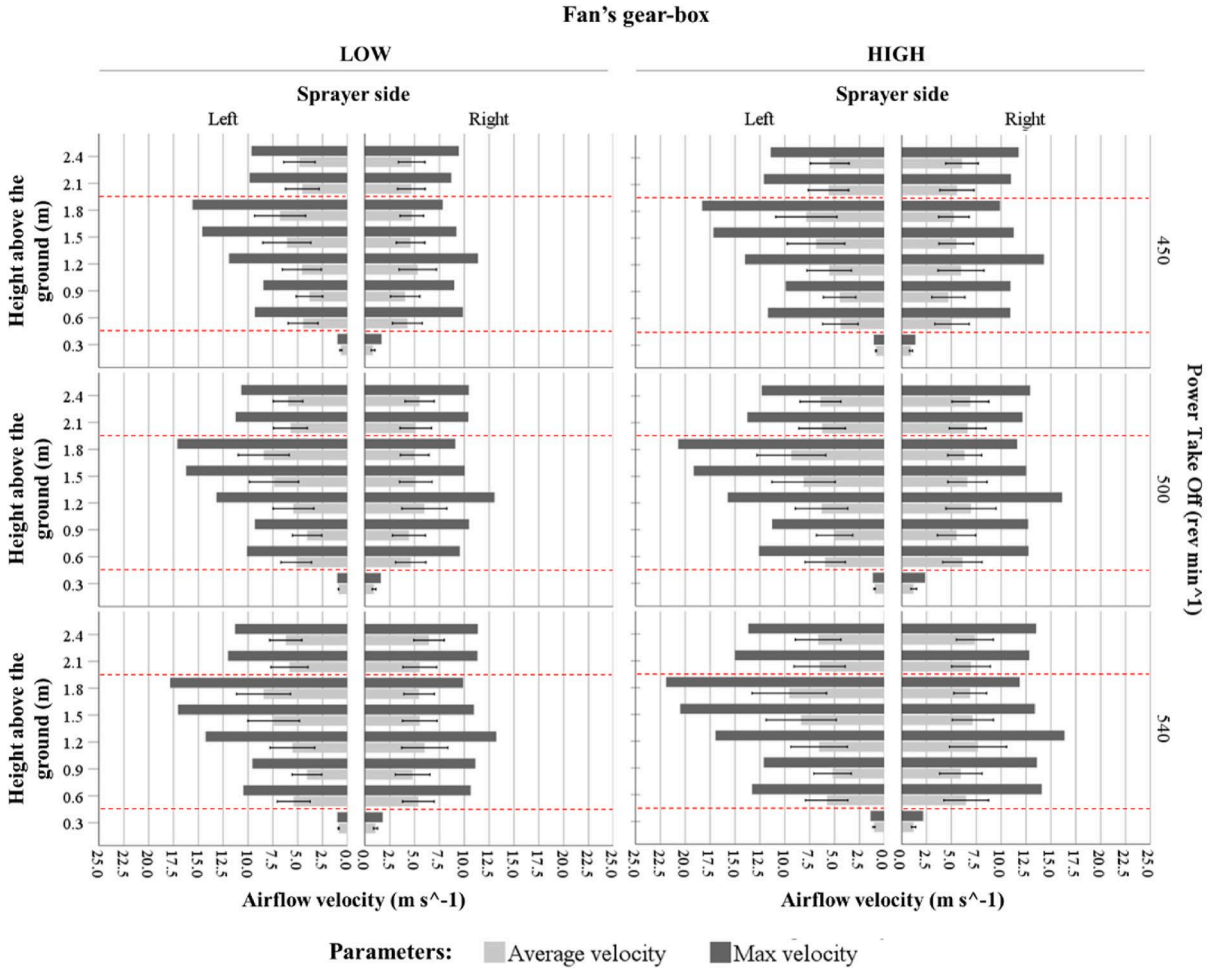

Fig. A3. Airflow velocity (m s^{-1}) at the target (1.25 m from the central axis of the sprayer) for the right and left sprayer side and for each combination of fan gear speed (low and high) and Power Take Off setting (450, 500 and 540 rev min^{-1}) at the orthogonal air-conveyor orientation. The red dashed lines represent the lower (0.5 m) and upper border (2.0 m) of the canopy target. The bars show the mean ± standard error of the mean.

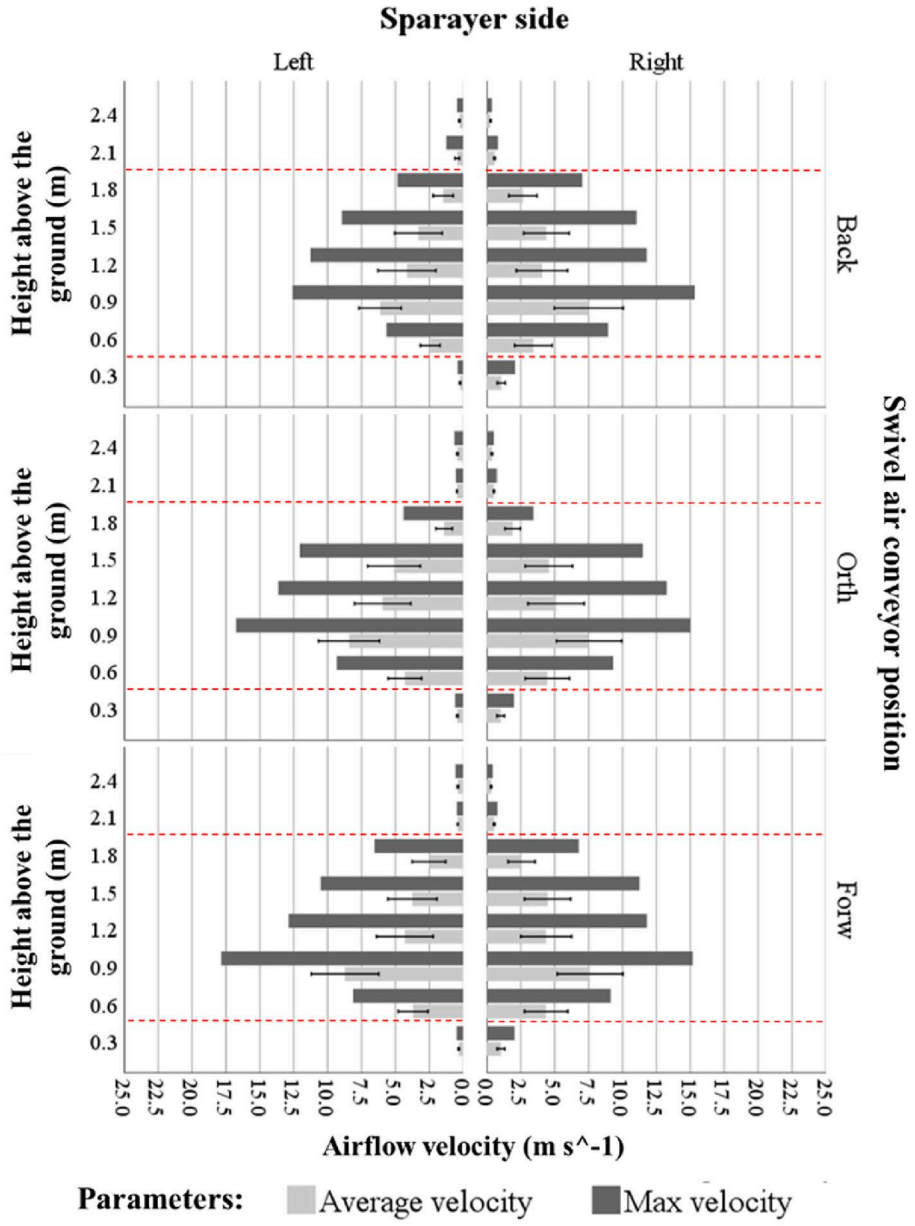

Fig. A4. Airflow velocity (m s^{-1}) at the target (1.25 m from the central axis of the sprayer) for the right and left sprayer side and for the different air-conveyor orientations (backward, orthogonal and forward). In all cases, the low fan gear speed, 450 rev min^{-1} Power Take Off, and the air deflectors properly adjusted to match the canopy target, were used. The red dashed lines represent the lower (0.5 m) and upper border (2.0 m) of the canopy target. The bars show the mean ± standard error of the mean.

References

Badules, J., Vidal, M., Boné, A., Llop, J., Salcedo, R., Gil, E., García-Ramos, F.J., 2018. Comparative study of CFD models of the air flow produced by an air-assisted sprayer adapted to the crop geometry. Comput. Electron. Agric. 149, 166–174.

Bahlol, H.Y., Chandel, A.K., Hoheisel, G.A., Khot, L.R., 2019. Smart spray analytical system for orchard sprayer calibration: a-proof-of-concept and preliminary results. Trans. ASABE (Am. Soc. Agric. Biol. Eng.) 63, 29–35.

Bahlol, H.Y., Chandel, A.K., Hoheisel, G.A., Khot, L.R., 2020. The smart spray analytical system: developing understanding of output air-assist and spray patterns from orchard sprayers. Crop. Protect. 127, 104977.

Balsari, P., Marucco, P., 2004. Sprayer adjustment and vine canopy parameters affecting spray drift: the Italian experience. In: Paper Presented at the International Conference on Pesticide Application for Drift Management, Waikoloa, Hawaii.

Balsari, P., Marucco, P., Oggero, G., Tamagnone, M., 2008. Study of optimal air velocities for pesticide application in vineyard. Aspect Appl. Biol. 84, 417–424.

Balsari, P., Grella, M., Vitali, M., Marucco, P., 2018. Assessment of vineyard parameters enabling prediction of the volume effectively applied when using a recycling tunnel sprayer. Intern. adv. pesti. appli. - Asp. Appl. Biol. 137, 85–91.

Berk, P., Hocevar, M., Stajnko, D., Belsak, A., 2016. Development of alternative plant protection product application techniques in orchards, based on measurement sensing systems: a review. Comput. Electron. Agric. 124, 273–288.

Biocca, M., Gallo, P., 2014. Comparison between horizontal and vertical lamellate patternators for air-blast sprayers. Open Agric. J. 8, 12–17.

Butler Ellis, M.C., Lane, A.G., O'Sullivan, C.M., Miller, P.C.H., Glass, C.R., 2010. Bystander exposure to pesticide spray drift: new data for model development and validation. Biosyst. Eng. 107, 162–168.

Campos, J., Llop, J., Gallart, M., Garcìa-Ruiz, F., Gras, A., Salcedo, R., Gil, E., 2019. Development of canopy vigour maps using UAV for site-specific management during vineyard spraying process. Precis. Agric. 20, 1136–1156.

Cerruto, E., 2007. Influence of airflow rate and forward speed on the spray deposit in vineyards. J. Agric. Eng. 1, 7–14.

Codis, S., Verges, A., Auvergne, C., Bonicel, J.F., Diouloufet, G., Cavalier, R., Douzals, J. P., Magnier, J., Montegano, P., Ribeyrolles, X., Ruelle, B., 2015. Optimization of early growth stage treatments of the vine: experimentations on the artificial vine EvaSprayViti. In: Proceeding of SUPROFRUIT 2015 - 13th Workshop on Spray Application in Fruit Growing, 15-18 July 2015, Lindau - DE, pp. 47–48.

Comba, L., Zaman, S., Biglia, A., Ricauda Aimonino, D., Dabbene, F., Gay, P., 2020. Semantic interpretation and complexity reduction of 3D point clouds of vineyards. Biosyst. Eng. 197, 216–230. https://doi.org/10.1016/j.biosystemseng.2020.05.013.

Cross, J.V., Walklate, P.J., Murray, R.A., Richardson, G.M., 2003. Spray deposits and losses in different sized apple trees from an axial fan orchard sprayer: 3. Effects of air volumetric flow rate. Crop. Protect. 22 (2), 381–394.

Dekeyser, D., Duga, A.T., Verboven, P., Endalew, A.M., Hendrickx, N., Nuyttens, D., 2013. Assessment of orchard sprayers using laboratory experiments and computational fluid dynamics modelling. Biosyst. Eng. 114 (2), 157–169.

Dekeyser, D., Foqué, D., Duga, A.T., Verboven, P., Hendrickx, N., Nuyttens, D., 2014. Spray deposition assessment using different application techniques in artificial orchard trees. Crop. Protect. 64, 187–197.

Delele, M.A., Jaeken, P., Debaer, C., Baetens, K., Endalew, A.M., Ramon, H., Nicolaï, B. M., Verboven, P., 2007. CFD prototyping of an air-assisted orchard sprayer aimed at drift reduction. Comput. Electron. Agric. 55 (1), 16–27. https://doi.org/10.1016/j.compag.2006.11.002.

Deng, W., Zhao, C., Zhou, J., 2020. Comparison and evaluation of spray characteristics of three types of variable-rate spray. In: Proceeding of Virtual ICPA –International Conference on Precision Agriculture- 2020, 2nd April 2021. https://www.ispag.org/abstract_papers/papers/abstract_1087.pdf.

Doruchowski, G., Balsari, P., van de Zande, J., 2009. Development of a crop adapted spray application system for sustainable plant protection in fruit growing. Acta Hortic. 824, 251–260. https://doi.org/10.17660/ActaHortic.2009.824.29.

EC, 2020. European Commission - Farm to Fork Strategy - for a Fair, Healthy and Environmentally-Friendly Food System. https://ec.europa.eu/food/farm2fork_en. (Accessed 2 April 2020).

Farooq, M., Landers, A., 2004. Interactive effects of air, liquid and canopies on spray patterns of axial-flow sprayers. In: Paper Presented at the ASAE/CSAE Annual International Meeting, Ottawa, Ontario, Canada, 1-4 August.

Farooq, M., Salyani, M., 2002. Spray penetration into the citrus tree canopy from two air-carrier sprayers. Trans. ASAE (Am. Soc. Agric. Eng.) 45 (5), 1287–1293.

Felsot, A.S., Unsworth, J.B., Linders, J.B.H.J., Roberts, G., 2011. Agrochemical spray drift; assessment and mitigation – a review. J. Environ. Sci. Health B 46, 1–23.

Friso, D., Baldoin, C., Pezzi, F., 2015. Mathematical modeling of the dynamics of air jet crossing the canopy of tree crops during pesticide application. Appl. Math. Sci. 9 (26), 1281–1296.

Garcerá, C., Moltó, E., Chueca, P., 2017. Spray pesticide applications in Mediterranean citrus orchards: canopy deposition and off-target losses. Sci. Total Environ. 599, 1344–1362.

Gil, E., Escolà, A., Rosell, J.R., Planas, S., Val, L., 2007. Variable rate application of plant protection products in vineyard using ultrasonic sensors. Crop. Protect. 26, 1287–1297.

Gil, E., Landers, A., Gallart, M., Llorens, J., 2013. Development of two portable patternators to improve drift control and operator training in the operation of vineyard sprayers. Span. J. Agric. Res. 11 (3), 615–625. https://doi.org/10.5424/sjar/2013113-3638.

Gil, E., Gallart, M., Gioelli, F., Balsari, P., Koutsouris, A., Codis, S., Nuyttens, D., Fountas, S., 2020. INNOSETA - an H2020 European project to fill the gap between research and professional users in crop protection. International advances in pesticide application - Asp. Appl. Biol 144, 211–220.

Giles, D.K., Comino, J.A., 1989. Variable flow control for pressure atomization nozzles. SAE Trans. 98 (2).

Godyn, A., Doruchowski, G., Swiechowski, W., Holownicki, R., 2014. The influence of nozzle configuration in orchard sprayers on the vertical distribution of spray. Agric. Eng. 4 (152), 71–80. https://doi.org/10.14654/ir.2014.152.082.

Grella, M., Gallart, M., Marucco, P., Balsari, P., Gil, E., 2017. Ground deposition and airborne spray drift assessment in vineyard and orchard: the influence of environmental variables and sprayer settings. Sustainability 9, 728. https://doi.org/10.3390/su9050728.

Grella, M., Marucco, P., Balsari, P., 2019. Toward a new method to classify the airblast sprayers according to their potential drift reduction: comparison of direct and new indirect measurement methods. Pest Manag. Sci. 75, 2219–2235. https://doi.org/10.1002/ps.5354.

Grella, M., Miranda-Fuentes, A., Marucco, P., Balsari, P., 2020. Field assessment of a newly-designed pneumatic spout to contain spray drift in vineyards: evaluation of canopy distribution and off-target losses. Pest Manag. Sci. 76 (12), 4173–4191. https://doi.org/10.1002/ps.5975.

Grella, M., Gioelli, F., Marucco, P., Zwertvaegher, I., Mozzanini, E., Mylonas, N., Nuyttens, D., Balsari, P., 2021. Field assessment of a pulse width modulation spray system applying different spray volumes: duty cycle and forward speed effects on vines spray coverage. Precis. Agric. https://doi.org/10.1007/s11119-021-09835-6 (in press).

Hislop, E.C., 1991. Air-assisted crop spraying: an introductory review. In: Proceedings of BCPC Symposium on Air-Assisted Spraying in Crop Protection, 7-9 January, Swansea, UK, pp. 3–14.

Hoheisel, G.-A., Khot, L.R., Moyer, M., Castagnoli, S., 2020. PNW749 Six Steps to Calibrate and Optimize Airblast Sprayers. Pacific North West Extension Publications.

Hołownicki, R., Doruchowski, G., Swiechowski, W., Godyn, A., Konopacki, P.J., 2017. Variable air assistance system for orchard sprayers; concept, design and preliminary testing. Biosyst. Eng. 163, 134–149.

Intrieri, C., Poni, S., 1995. Integrated evolution of trellis training systems and machines to improve grape quality and vintage quality of mechanized Italian vineyards. Am. J. Enol. Vitic. 46, 116–127.

Kasner, E.J., Fenske, R.A., Hoheisel, G.A., Galvin, K., Blanco, M.N., Seto, E.Y., Yost, M.G., 2020. Spray drift from three airblast sprayer technologies in a modern orchard work environment. Ann. Work Expos. Heal. 64, 25–37.

Lander, A., 2010. Improving spray deposition and reducing drift – airflow adjustment is the answer. New York. Fruit. Quarter. 19 (4), 3–6.

Li, L., He, X., Song, J., Liu, Y., Zeng, A., Yang, L., Liu, C., Liu, Z., 2018. Design and experiment of variable rate orchard sprayer based on laser scanning sensor. Int. J. Agric. Biol. Eng. 11, 101–108.

Li, J., Li, Z.Q., Ma, Y.K., Cui, H.J., Yang, Z., Lu, H.Z., 2021. Effects of leaf response velocity on spray deposition with an air-assisted orchard sprayer. Int. J. Agric. Biol. Eng. 14 (1), 123–132.

Llorens, J., Gil, E., Llop, J., Escolà, A., 2010. Variable rate dosing in precision viticulture: use of electronic devices to improve application efficiency. Crop. Protect. 29, 239–248.

Lorenz, D., Eichorn, D., Bleiholder, H., Klose, R., Meier, U., Weber, E., 1995. Phenological stages of development of the grapevine (*Vitis vinifera* L. ssp. *Vinifera*). Coding and description according to the expanded BBCH scale. Aust. J. Grape Wine Res. 1 (2), 100–103. https://doi.org/10.1111/j.1755-0238.1995.tb00085.x.

Mammarella, M., Comba, L., Biglia, A., Dabbene, F., Gay, P., 2020. Cooperative agricultural operations of aerial and ground unmanned vehicles. IEEE Intern. Work. Metrol. Agricul. Fores. MetroAgri. For 9277573, 224–229. https://doi.org/10.1109/MetroAgriFor50201.2020.9277573.

Marucco, P., Tamagnone, M., Balsari, P., 2008. Study of air velocity adjustment to maximise spray deposition in peach orchards. In: Agricultural Engineering International: the CIGR Ejournal, X(ALNARP 08 009).

Marucco, P., Balsari, P., Grella, M., Pugliese, M., Eberle, D., Gil Moya, E., Llop Casamada, J., Fountas, S., Mylonas, N., Tsitsigiannis, D., Balafoutis, A., Polder, G., Nuyttens, D., Dias, L., Douzals, J.P., 2019. OPTIMA EU project: main goal and first results of inventory of current spray practices in vineyards and orchards. In: Proceeding of SUPROFRUIT 2019 - 15th Workshop on Spray Application and Precision Technology in Fruit Growing, 16-18 July 2019, East Malling - UK, pp. 99–100.

Miller, P.R., Salyani, M., Hiscox, A.L., 2003. Remote measurement of spray drift from orchard sprayers using LIDAR. In: Proceeding of the American Society of Agricultural and Biological Engineers; 2003 July 27-20; NV, USA; Annual Meet Paper 031093.

Panneton, B., Lacasse, B., Piché, M., 2005. Effect of air-jet configuration on spray coverage in vineyards. Biosyst. Eng. 90 (2), 173–184.

Pascuzzi, 2016. Outcomes on the spray profiles produced by the feasible adjustments of commonly used sprayers in “tendone” vineyards of Apulia (southern Italy). Sustainability 8 (12), 1307.

Pascuzzi, S., Santoro, F., Manetto, G., Cerruto, E., 2018. Study of the correlation between foliar and patternator deposits in a “tendone” vineyard. Agric. Eng. Int. 20 (3), 97–107.

Pergher, G., 2004. Field evaluation of a calibration method for air-assisted sprayers involving the use of a vertical patternator. Crop. Protect. 23 (5), 437–446.

Pergher, G., 2006. The effect of airflow rate and forward speed on spray deposition from a vineyard sprayer. J. Agric. Eng. 1, 17–23.

Pergher, G., Petris, R., 2008. The effect of air flow rate on spray deposition in a guyot-trained vineyard. In: Agricultural Engineering International: the CIGR Ejournal. Manuscript ALNARP 08 010, X. May, 2008.

Pergher, G., Gubiani, R., Cividino, S.R., Dell’Antonia, D., Lagazio, C., 2013. Assessment of spray deposition and recycling rate in the vineyard from a new type of air-assisted tunnel sprayer. Crop. Protect. 45, 6–14.

Randall, J.M., 1971. The relationship between air volume and pressure on spray distribution in fruit trees. J. Agric. Eng. Res. 16, 1–31.

Rathnayake, A.P., Chandel, A.K., Schrader, M.J., Hoheisel, G.A., Khot, L.R., 2021. Spray patterns and perceptive canopy interaction assessment of commercial airblast sprayers used in Pacific Northwest perennial specialty crop production. Comput. Electron. Agric. 184, 106097.

Rautmann, D., Streloke, M., Winkler, R., 2001. New basic drift values in the authorization procedure for plant protection products. Mitt. aus der Biol. Bundes. fur Land - und. Forstwirtsch. 383, 133–141.

Salcedo, R., Garcera, C., Granell, R., Molto, E., Chueca, P., 2015a. Description of the airflow produced by an air-assisted sprayer during pesticide applications to citrus. Spanish J. Agric. Res. 13 (2).

Salcedo, R., Granell, R., Palau, G., Vallet, A., Garcerá, C., Chueca, P., Moltó, E., 2015b. Design and validation of a 2D CFD model of the airflow produced by an airblast sprayer during pesticide treatments of citrus. Comput. Electron. Agric. 116, 150–161.

Salcedo, R., Pons, P., Zaragoza, T., Campos, J., Ortega, P., Gallart, M., Gil, E., 2019. Dynamic evaluation of airflow stream generated by a reverse system of an axial fan sprayer using 3D-ultrasonic anemometers. Effect of canopy structure. Comput. Electron. Agric. 163, 104851 https://doi.org/10.1016/j.compag.2019.06.006.

Salcedo, R., Llop, J., Campos, J., Costas, M., Gallart, M., Ortega, P., Gil, E., 2020a. Evaluation of leaf deposit quality between electrostatic and conventional multi-row sprayers in a trellised vineyard. Crop. Protect. 127, 104964.

Salcedo, R., Zhu, H., Zhang, Z., Wei, Z., Chen, L., Ozkan, E., Falchieri, D., 2020b. Foliar deposition and coverage on young apple trees with PWM-controlled spray systems. Comput. Electron. Agric. 178, 105794.

Salcedo, R., Fonte, A., Grella, M., Garcerá, C., Chueca, P., 2021. Blade pitch and air-outlet width effects on the airflow generated by an airblast sprayer with wireless remote-controlled axial fan. Comput. Electron. Agric. 190, 106428 https://doi.org/10.1016/j.compag.2021.106428.

Sánchez-Hermosilla, J., Rincón, V.J., Páez, F., Fernández, M., 2012. Comparative spray deposits by manually pulled trolley sprayer and a spray gun in greenhouse tomato crops. Crop. Protect. 31, 119–124.

Svensson, S.A., 2001. Air jet influence on application results in orchards. Mat. Konf. Racjonalna Technika Ochrony Roślin 122–134.

Świechowski, W., Doruchowski, G., Hołownicki, R., Godyń, A., 2004. Penetration of air within the apple tree canopy as affected by the air jet characteristics and travel velocity of the sprayer. EJPAU 7 (2). http://www.ejpau.media.pl/volume7/issue2/engineering/art-03.html. (Accessed 2 July 2021).

TOPPS-Prowadis Project, 2014. Best management practices to reduce spray drift. Available at. http://www.topps-life.org/. (Accessed 2 January 2021).

Triloff, P., 2015. Results of measuring the air distribution of sprayers for 3D-crops and parameters for evaluating and comparing fan types. In: Proceeding of SUPROFRUIT 2015 - 13th Workshop on Spray Application Techniques in Fruit Growing , Lindau - DE, 15–18 July.

Triloff, P., 2016. Results and conclusions from five years measuring and adjusting air distribution of brand new sprayers for 3D-Crops. In: Proceeding of 6th European Workshop on Standard Procedure for the Inspection of Sprayers in Europe (SPISE), Castelldefels - ES, 13-15 September.

van de Zande, J.C., Schlepers, M., Hofstee, J.W., Michielsen, J.M.G.P., Wenneker, M., 2017. Characterization of the air-flow and the liquid distribution of orchard sprayers. In: Proceeding of SUPROFRUIT 2017 - 14th Workshop on Spray Application Techniques in Fruit Growing , Hasselt, Limburg, BE, 1-12 May..

Vereecke, E., Langenakens, J., De Moor, A., Pieters, M., Jaeken, P., 2000. The air distribution generated by air-assisted orchard sprayers. In: Proceeding of 52nd International Symposium on Crop Protection, Pts I and Ii, 65, pp. 991–1000, 2A-B.

Viret, O., Siegfried, W., Holliger, E., Raisigl, U., 2003. Comparison of spray deposits and efficacy against powdery mildew of aerial and ground-based spraying equipment in viticulture. Crop. Protect. 22 (8), 1023–1032.

Vitali, M., Tamagnone, M., La Iacona, T., Lovisolo, C., 2013. Measurement of grapevine canopy leaf area by using an ultrasonic-based method. J. Int. Sci. Vigne du Vin 47, 183–189. https://doi.org/10.20870/oenoo ne.2013.47.3.1553.

Wegener, J.K., von Hörsten, D., Pelzer, T., Osteroth, H.J., 2016. Basic research into different parameters influencing the quality of vertical distribution by crop sprayers. Landtechnik 71 (1), 4–13. https://doi.org/10.15150/lt.2016.3116.